THE JOURNAL OF COMPARATIVE NEUROLOGY 497:928–958 (2006)

Systematic Analysis of the Visual Projection Neurons of *Drosophila melanogaster*. I. Lobula-Specific Pathways

HIDEO OTSUNA[1–4] **AND KEI ITO**[1,3,4]*****

[1]Institute of Molecular and Cellular Biosciences (IMCB), University of Tokyo, Yayoi, Bunkyo-ku, Tokyo 113-0032, Japan
[2]Division of Biological Science, Nagoya University, Nagoya 464-8602, Japan
[3]National Institute for Basic Biology, Myodaiji, Okazaki, 444-8585 Aichi, Japan
[4]Institute for Bioinformatics Research and Development (BIRD), JST, c/o IMCB, University of Tokyo, Yayoi, Bunkyo-ku, Tokyo 113-0032, Japan

ABSTRACT

In insects, visual information is processed in the optic lobe and conveyed to the central brain. Although neural circuits within the optic lobe have been studied extensively, relatively little is known about the connection between the optic lobe and the central brain. To understand how visual information is read by the neurons of the central brain, and what kind of centrifugal neurons send the control signal from the central brain to the optic lobe, we performed a systematic analysis of the visual projection neurons that connect the optic lobe and the central brain of *Drosophila melanogaster*. By screening ~4,000 GAL4 enhancer-trap strains we identified 44 pathways. The overall morphology and the direction of information of each pathway were investigated by expressing cytoplasmic and presynapsis-targeted fluorescent reporters. A canonical nomenclature system was introduced to describe the area of projection in the central brain. As the first part of a series of articles, we here describe 14 visual projection neurons arising specifically from the lobula. Eight pathways form columnar arborization in the lobula, whereas the remaining six form tangential or tree-like arborization. Eleven are centripetal pathways, among which nine terminate in the ventrolateral protocerebrum. Terminals of each columnar pathway form glomerulus-like structures in different areas of the ventrolateral protocerebrum. The posterior lateral protocerebrum and the optic tubercle were each contributed by a single centripetal pathway. Another pathway connects the lobula on each side of the brain. Two centrifugal pathways convey signals from the posterior lateral protocerebrum to the lobula. J. Comp. Neurol. 497:928–958, 2006.

Indexing terms: *Drosophila*; insect; visual projection neuron; arborization; optic lobe; central brain; GAL4 enhancer trap

Vision is of prime importance for many animal species to obtain vital information about the ambient environment and nearby objects. In spite of their apparent morphological differences, vertebrate and insect visual systems share many essential features. The signal of the incoming light is detected by an array of photoreceptors in the eyes and transmitted to lower visual centers in the brain, where the retinotopic projection map is maintained. Visual information is then conveyed further to various higher processing sites, where retinotopic arrangements are no longer obvious in many cases.

In insects, a compound eye consists of an array of ommatidia, each of which comprises a lens and a distinct number of photoreceptor cells. In case of the fruit fly *Drosophila melanogaster*, there are ~780 and 730 ommatidia in an eye of a female and male fly, respectively (Wolff and Ready, 1993). Each ommatidium houses eight photoreceptor cells (R1–R8). The photoreceptor cells R1–R6 ex-

This article includes Supplementary Material, which is available online at http://www.interscience.wiley.com/jpages/0021-9967/suppmat.

Grant sponsor: Institute for Bioinformatics Research and Development (BIRD) / Japan Science and Technology Agency (JST); Grant sponsor: Grant-in-Aid for Scientific Research from the Ministry of Education, Culture, Sports, Science and Technology of Japan (to K.I.).

*Correspondence to: Kei Ito, Institute of Molecular and Cellular Biosciences, University of Tokyo, Yayoi, Bunkyo-ku, Tokyo 113-0032, Japan. E-mail: itokei@iam.u-tokyo.ac.jp

Received 17 August 2005; Revised 6 January 2006; Accepted 6 February 2006

DOI 10.1002/cne.21015

Published online in Wiley InterScience (www.interscience.wiley.com).

press the gene RH1, which is mainly sensitive to a wide range of wavelengths, from ultraviolet (UV) to orange-red, with the peak sensitivity to blue light (Salcedo et al., 1999). The photoreceptor R7 expresses either RH3 or RH4, which is mainly sensitive to UV light (Feiler et al., 1992). The R8 expresses either RH5 or RH6, which is sensitive to blue or green light, respectively (Salcedo et al., 1999).

Whereas a vertebrate eye contains an intense neural network within its retina, insect photoreceptor cells project directly to the primary visual center of the brain, the optic lobe. The optic lobe consists of three or four neuropils. The lamina, medulla, and lobula are distinguishable in all the insect species. In insects such as flies, butterflies, and moths, the lobula is further separated into two neuropils, which are called the lobula and lobula plate (Sinakevitch et al., 2003) (Fig. 1). The axons of six photoreceptor cells (R1–R6) from neighboring ommatidia intertwine with each other and collectively terminate in the lamina (Meinertzhagen and Hanson, 1993). Axons of R7 and R8 cells pass through the lamina and terminate directly in the medulla (Fig. 1C).

Local neurons, interneurons, and the terminals of the photoreceptors that are oriented to the identical direction form a columnar organization called the visual cartridge, whose spatial organization reflects that of the ommatidia (white lines in Fig. 1A,B). Lamina interneurons (second-order neurons) innervate the medulla and terminate in the cartridges covering the corresponding visual field. Columnar interneurons of the medulla (second-, third-, or fourth-order neurons) then project to the lobula and lobula plate, in which the retinotopic arrangements of the visual cartridges are also maintained (Strausfeld, 1976; Fischbach and Dittrich, 1989).

In the medulla, lobula, and lobula plate, the arborization of columnar neurons and the innervation of tangential neurons form a layered organization that is perpendicular to the direction of the visual cartridges (Fig. 1A,B). Photoreceptors R1–6, R7, and R8 and their associated interneurons arborize at distinct layers in each neuropil (Fischbach and Dittrich, 1989; Strausfeld and Lee, 1991; Bausenwein et al., 1992) (Fig. 1C). For example, the UV-sensitive R7 cells form extensive arborization in the M6 layer of the medulla, whereas blue/green-sensitive R8 cells terminate in its M3 layer. Certain medulla interneurons preferentially connect these layers to the M8 layer in the medulla and Lo4-6 layers in the lobula (Bausenwein and Fischbach, 1992).

There are four classes of neurons that form the neural circuits in the optic lobe: photoreceptor axons, intrinsic neurons (or local neurons), interneurons, and visual projection neurons (VPNs). Intrinsic neurons arborize within a single optic neuropil, interneurons connect more than one neuropil within the optic lobe, and VPNs connect the optic lobe and the central brain.

Neurons in the insect optic lobe are reported to extract characteristic features of the visual information, such as brightness and motion. The VPNs should convey such information to higher visual centers in the central brain. For example, electrophysiological and Ca^{2+} dynamics imaging analyses of the brains of the butterfly *Papilio aegeus*, moth *Manduca sexta*, house fly *Musca domestica*, and the blowfly *Calliphora erythrocephala* showed that certain VPNs deriving from medulla and lobula plate respond only to motion of distinct angles (Ibbotson et al., 1991; Gilbert and Strausfeld, 1992; Milde, 1993; Strausfeld et al., 1995; Douglass and Strausfeld, 1996; Krapp and Hengstenberg, 1996; Single and Borst, 1998; Egelhaaf and Warzecha, 1999; Krapp et al., 2001; Haag and Borst, 2004; Kalb et al., 2004). VPNs are also involved in various other kinds of visual processing such as the detection of looming or receding objects (Wicklein and Strausfeld, 2000) and polarized light (Homberg and Würden, 1997; Loesel and Homberg, 2001) as well as the control of the circadian rhythm (Renn et al., 1999).

Compared with the optic lobe interneurons (mostly second-, third-, and fourth-order neurons) and local neurons, relatively little is known about the structures of the VPNs (mostly third-, fourth-, and fifth-order neurons). Although VPNs have been described in various insect species (Strausfeld, 1991, 1976; Strausfeld and Hausen, 1977; Fischbach and Dittrich, 1989; Hausen and Egelhaaf, 1989; Ibbotson et al., 1991; Meinertzhagen and Hanson, 1993; Milde, 1993; Wicklein and Strausfeld, 2000; Haag and Borst, 2001; Loesel and Homberg, 2001; Douglass and Strausfeld, 2003), information about the detailed 3D morphology of the VPNs is scarce.

In order to understand how visual information preprocessed in the optic lobe is read by the neurons in the higher visual centers of the central brain, and what kind of centrifugal neurons send the control signal from the central brain to the optic lobe, it is very important to understand the systematic wiring patterns of the VPNs. To this aim, we performed a large-scale screening of *Drosophila* GAL4 enhancer-trap strains that label specific subsets of VPNs. By expressing cytoplasmic reporter protein such as the green fluorescent protein (GFP) under the control of the GAL4 target sequence UAS (Brand and Perrimon, 1993), the overall morphology of the labeled cells was visualized. By screening a collection of about 4,000 GAL4 enhancer-trap strains we identified a total of 44 VPN pathways.

As the first part of a series of articles describing these neurons, we here report the systematic identification and classification of VPNs that specifically connect the lobula and the central brain. VPNs that contribute not only to lobula but also to lobula plate and/or medulla will be reported in a separate article (Part II). VPNs associated specifically with the lobula plate and medulla will be published subsequently (Parts III and IV).

MATERIALS AND METHODS

Fly strains

To label specific neurons in the visual pathway, we screened 3,939 GAL4 enhancer-trap strains. Among them 383 lines (MZ series) were originally generated by J. Urban and colleagues at the laboratory of G.M. Technau (Ito et al., 1995), and 3,556 lines (NP series) were made by the NP consortium, a joint venture of eight fly laboratories in Japan (Yoshihara and Ito, 2000; Hayashi et al., 2002). The MZ series were generated by crossing pGawB (Brand and Perrimon, 1993) and P[ry^+; $\Delta 2-3$] (99B) strains (Robertson et al., 1988). NP series were generated using a kit of strains that features a pGawB strain in a different locus than the original strain and P[ry^+; $\Delta 2-3$] and balancer strains on a newly established isogenized *Canton S* background (Yoshihara and Ito, 2000). Compared to the original pGawB strain reported by Brand and Perrimon (1993), the kit has a higher efficiency of pGawB transposon jump

to new genetic loci. Using this kit, each laboratory of the NP consortium generated about 500 strains and pooled the lines for common use (Hayashi et al., 2002). The collection of NP strains is available via the Kyoto Stock Center (*Drosophila* Genetic Resource Center, Kyoto Institute of Technology, http://www.dgrc.kit.ac.jp/en/) and the NIG stock center (National Institute of Genetics, http://www.shigen.nig.ac.jp/fly/nigfly/). Information on the insertion site of each GAL4 strain is available at the GETDB database (http://flymap.lab.nig.ac.jp/getdb.html). The list of strains used in this study is summarized in Table 2.

Three UAS-linked reporter strains were used for visualizing GAL4-expressing cells. A strain carrying cytoplasmic UAS-*GFP S65T* (T2 strain, gift from Barry Dickson) was used most often (Figs. 4–13, 15, 16). A strain carrying both GFP fused with neuronal synaptobrevin (UAS-*n-syb::GFP*) (Ito et al., 1998; Estes et al., 2000) and red fluorescent protein DsRed S197Y (UAS-*DsRed*) (Verkhusha et al., 2001) were used for visualizing the distribution of the presynaptic sites and the overall cell morphology simultaneously (Figs. 4D,E, 14).

Flies were raised at 25°C under a 12/12-hour light/dark cycle. Brains of female flies at 5–10 days after eclosion were observed. Flies younger than 5 days were avoided because in these flies reporter expression was sometimes detected in cells that do not express GAL4 in older, mature flies. This is probably because GAL4 proteins expressed under the influence of the enhancer activity during pupal stages would remain active for a certain period after eclosion.

Imaging and 3D reconstruction

For the first screening, the 3,939 GAL4 enhancer-trap strains were crossed with the UAS-*GFP S65T* (T2) strain. Adult brains were dissected in phosphate-buffered saline (PBS, pH 7.4 at 25°C) and observed directly without fixation. For more detailed analyses, brains were dissected in PBS and fixed with 4% formaldehyde in PEM (100 mM PIPES, 2 mM EGTA, 1 mM $MgSO_4$) for 2 hours at 4°C. Samples were rinsed with PBS, incubated with 50% glycerol in PBS for 2 hours or overnight, and cleared with 80% glycerol for fluorescence microscopy (Merck, Darmstadt, Germany) in PBS and mounted in the same solution.

Serial confocal optical sections at 1.3-μm intervals were taken with LSM 510 confocal microscopes (Karl Zeiss) and water-immersion 40× Plan-Apochromat objectives (n.a. = 1.2). In most cases, frontal (coronal) sections were taken from the posterior side of the brain. Because we had to

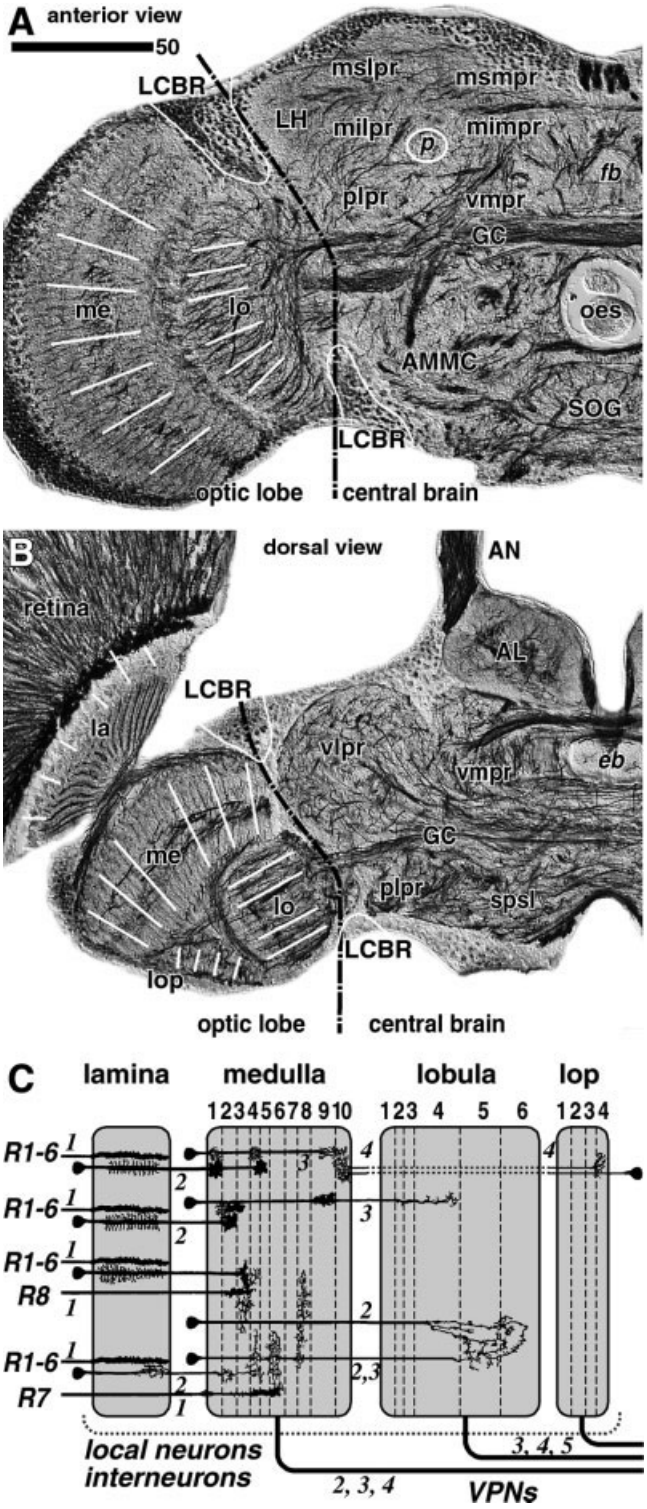

Fig. 1. Organization of the *Drosophila* visual system. **A,B:** Frontal (A) and horizontal (B) silver-stained paraffin sections showing the neuropil areas of the optic lobe and the central brain. Black dotted line indicates the border between the optic lobe and the central brain. White straight lines show the direction of the visual cartridges. White curved lines indicate the contour of the lateral cell body region (LCBR). **C:** Examples of the visual neurons in the optic lobe. Modified from Fischbach and Dittrich (1989). The numbers above the diagram indicate the numbers of the layers of each neuropil. The numbers in italics indicate the order of neurons counted from the photoreceptor cells (first-order neurons). Visual projection neurons (VPNs) link the medulla, lobula, and lobula plate with the central brain. la, lamina; me, medulla; lo, lobula; lop, lobula plate; LCBR, lateral cell body region; mslpr, middle superiorlateral protocerebrum; msmpr, middle superiormedial protocerebrum; milpr, middle inferiorlateral protocerebrum; mimpr, middle inferiormedial protocerebrum; plpr, posteriorlateral protocerebrum; vmpr, ventromedial protocerebrum; vlpr, ventrolateral protocerebrum; spsl, superior posterior slope; GC, great commissure; LH, lateral horn; AMMC, antennal mechanosensory and motor center; AN, antennal nerve; AL, antennal lobe; SOG, suboesophageal ganglion; oes, oesophagus; fb, fan shaped body; eb, ellipsoid body; p, pedunculus of the mushroom body. Scale bar = 50 μm.

take between 120 and 200 serial sections for each sample, which takes 20–30 minutes to complete, the resolution of a single section had to be limited to 512 × 512 pixels in order to minimize the effect of photobleaching.

The confocal dataset was subjected to 3D reconstruction (Figs. 4–16) using Imaris 2.7 software (BitPlane) running on Silicon Graphics Octane2 workstations using the "ray-tracing" algorithm with the transparency parameter set at 80–97%, depending on the condition of the dataset. For visualizing the morphology of individual neurons, the ray-tracing algorithm turned out to be superior to other methods such as maximum intensity, averaging, or iso-surface extraction.

The size, contrast, and brightness of the resulting images were adjusted with Photoshop 7.0 (Adobe Systems, San Jose, CA). In a few cases where the reconstructed images were further magnified, images were sharpened using the unsharp mask function.

To generate virtual reality movies (available as Supplemental data), with which one can observe the reconstructed neurons from any desired viewing angle, the confocal datasets were processed using Volocity 3.0 (Improvision) running on Power Macintosh computers.

Erasure of other labeled cells than the VPNs

To visualize the morphology of the selected VPNs more clearly, we erased the signals of other labeled cells from the confocal data. To do this efficiently, a series of TIFF-format images taken with the Zeiss LSM510 confocal microscope was imported to ImageReady software (Adobe) running on Macintosh computers, where each image of the confocal serial sections was assigned to a distinct layer. By viewing through neighboring layers (i.e., sections), the cell bodies and fibers of the labeled VPNs and other labeled cells were distinguished. In each section, signals attributed to the latter category were selected and painted in black (i.e., background color). The resulting image series was saved in TIFF format, imported to Imaris 2.7, and subjected to 3D reconstruction.

In some sections only a tiny cross section of a thin fiber could be attributed to the labeled VPNs. Care was taken not to lose track of such signals. Although it is relatively easy to erase unwanted neural fibers in the central brain, in some cases neural fibers in the optic lobe are so intermingled that erasing unwanted fibers might affect the signal of the fibers we want to visualize. In such a case the fibers of the unwanted cells in the lobula were kept untouched.

Identification of the neuropil areas

To visualize the structure of the neuropils, previous studies used antibodies like nc82 and BP101, which label synaptic areas. These markers, however, cannot visualize the neuropil areas that are occupied with bundles and tracts of neural fibers where synapses are absent, such as the anterior and posterior optic tracts.

To identify the organization of the tracts and neuropils regardless of synapses, we used the GAL4 strain NP1502, which labels a large subset of the cortex-associated glia and neuropil-associated glia (Ito et al., 1995). When cytoplasmic GFP is expressed using this GAL4 strain, glial processes are visualized clearly. Because areas that are packed with neural fibers are relatively devoid of glial processes, neuropils appear dark in the confocal sections (see Supplemental data). Borders between certain neuropils are clearly separated by a glial sheath, making it easier to discern the neuropil structure. Cortex is labeled densely, because cortex-associated glial cells send extensive processes between neural cell bodies. Using these cues, neuropil areas were selected and painted in the frontal, horizontal, and sagittal cross sections using Amira 3.1 Software. The painted areas were then divided into blocks using the positions of the great commissure and the mushroom body as landmarks (see the first section of Results as well as Supplemental data).

RESULTS

In the first six sections we explain the technical aspects employed for visualizing and analyzing VPNs. Then we report the structure of the identified VPNs.

Canonical naming system of the central brain regions

Unlike in the optic lobe, most of the central brain neuropil is not separated clearly into delineated regions. Only three particular regions in the central brain, the antennal lobe (AL), mushroom body (MB), and central complex (CC), are clearly separated from other neuropil regions by glial sheaths. The rest of the brain is often called collectively "diffused neuropils," because glial borders are not prominent and neural fibers do not form a clearly distinguishable unit structure. These neuropils have traditionally been divided into several areas according to their relative locations: superior medial protocerebrum (smpr), superior lateral protocerebrum (slpr), inferior medial protocerebrum (impr), inferior lateral protocerebrum (ilpr), ventrolateral protocerebrum (vlpr), and posterior slope (psl) (Strausfeld, 1976). The volume of each region is rather large, especially along the longitudinal axis, making it difficult to precisely describe the area of innervation within the central brain. The borders between the regions have not been defined explicitly. This has caused a problem when one wants to refer to a precise location of the brain unambiguously.

To document the areas of projection targets of the identified neurons like VPNs, a more detailed and reliable system is required. For this purpose, we introduced a systematic way to divide the brain neuropils other than the AL, MB, and CC into small blocks, the borders of which are precisely defined using easily identifiable landmarks (Figs. 2, 3; see also Supplemental data). The system will be used consistently in our subsequent articles. (Note that the purpose of this terminology is to establish an unambiguous way to describe the location in the central brain. The subdivisions may not have any correlation with functional brain units or circuitry modules. See Discussion for details.)

First, we divided the protocerebrum into three dorsoventral layers: superior, inferior, and ventral (blue lines in Fig. 2A,C). The horizontal plane that passes at the 50% height between the ventral edge of the pedunculus and the tip of the MB vertical lobe (α lobe), which is almost the same height as the dorsalmost apex of the brain, defines the border between the superior and inferior protocerebra (Fig. 2C). The plane that passes through the ventral edge of the MB pedunculus was chosen as the border that divides the inferior and ventral protocerebra (Fig. 2C). Note that the axis of the pedunculus is slanted by ~7–15%

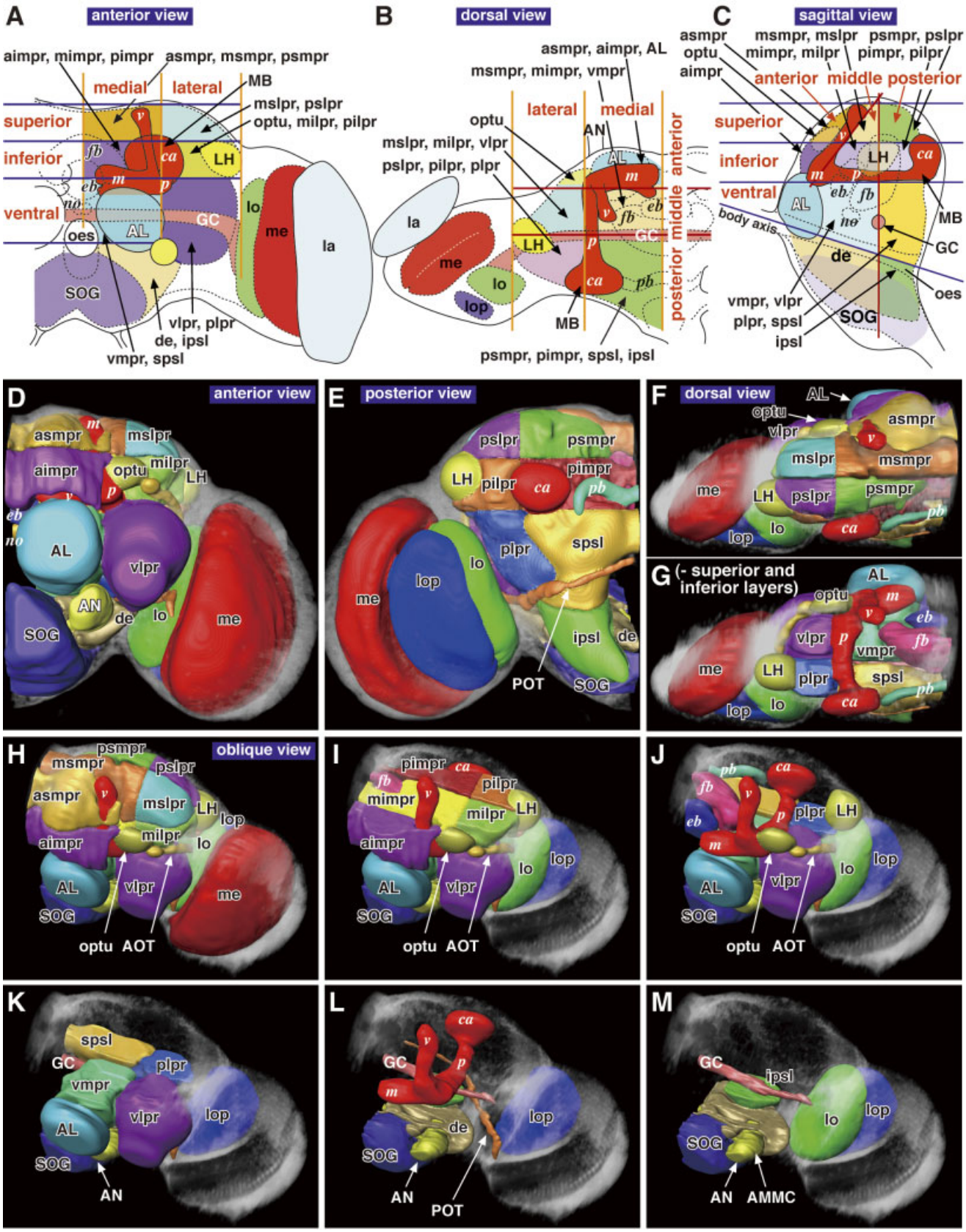

Fig. 2. Canonical naming system of the central brain regions. **A–C:** Schematic drawing of the brain viewed anteriorly (A), dorsally (B), and sagittally (C). Blue, orange, and red lines indicate the horizontal, sagittal, and coronal planes we used to divide the brain. **D–M:** Schematic 3D reconstruction of the brain regions viewed from the anterior (D), posterior (E), dorsal (F,G), and oblique (H–M) directions. In G and I–M, neuropil blocks in the dorsal areas are sequentially removed to show the blocks that lie in the more ventral areas of the brain. la, lamina; me, medulla; lo, lobula; lop, lobula plate; a-, anterior; m-, middle; p-, posterior; -s-, superior; -i-, inferior; v-, ventral; -lpr, lateral protocerebrum; -mpr, medial protocerebrum; optu, optic tubercle; de, deutocerebrum; psl, posterior slope; oes, oesophagus; GC, great commissure; AL, antennal lobe; SOG, suboesophageal ganglion; LH, lateral horn; MB, mushroom body (ca, calyx; p, pedunculus; m, medial lobe; v, vertical lobe); CC, central complex (fb, fan-shaped body; eb, ellipsoid body; no, noduli; pb, protocerebral bridge).

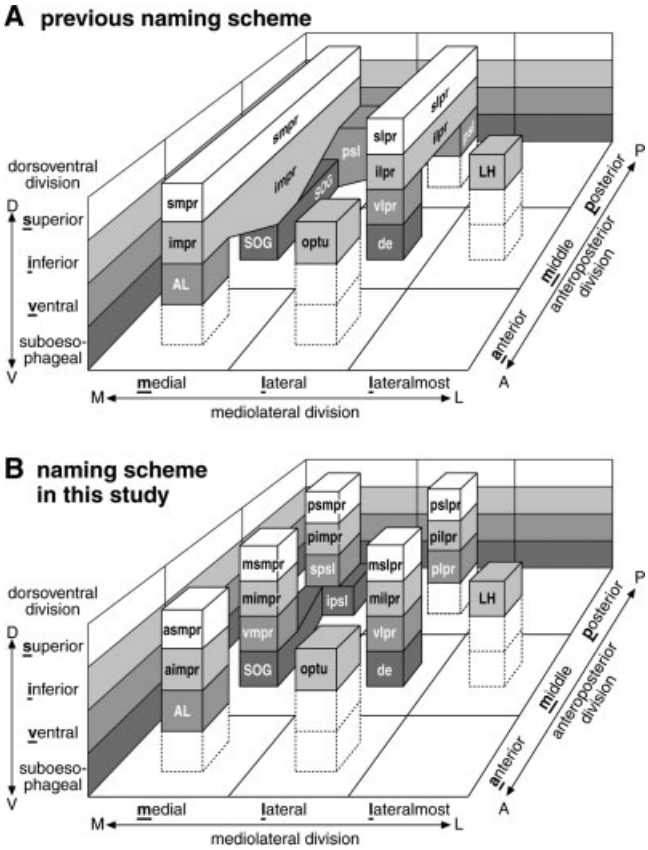

Fig. 3. Comparison of the previous naming scheme (**A**) and the naming system employed in this study (**B**). Abbreviations as in Figure 2

compared to the oesophageal foramen, which is the generally used landmark of the longitudinal brain axis. In spite of this, we chose the axis of the MB as the primary landmark, because 1) it is directly within the protocerebral area to be subdivided, making it easier to compare the spatial relationship; and 2) the location of the pedunculus is easily detectable using various markers and even without staining by observing the specimen using Nomarski optics (Tanaka et al., 2004).

Mediolaterally, we divided the central brain into medial and lateral protocerebra (orange lines in Fig. 2A,B). The sagittal plane that passes through the lateral edge of the pedunculus was chosen as the border between the medial and lateral regions.

Longitudinally, the central brain was divided into anterior, middle, and posterior protocerebra (red lines in Fig. 2C). The plane that passes through the posterior edge of the MB vertical lobe (α lobe) was taken as the border between anterior and middle protocerebra, and the plane that passes through the center of the great commissure (GC) and is perpendicular to the pedunculus was taken as the border between middle and posterior protocerebra. Because the former plane is inclined posteriorly, the protocerebral region between the two planes (i.e., middle protocerebrum) has a trapezoidal shape.

Using these five planes, the central brain neuropil other than the AL, MB, and CC is divided into 16 blocks (Figs. 2, 3). The area previously called smpr is subdivided into three regions: anterior smpr (asmpr), middle smpr (msmpr), and posterior smpr (psmpr, Figs. 2F,H, 3B). The slpr is divided into two regions: the middle slpr (mslpr) and posterior slpr (pslpr). Because there is essentially no neuropil that is anterior lateral to the MB vertical lobe, the anterior slpr does not exist (Figs. 2H, 3B).

Similarly, the impr was divided into anterior, middle, and posterior impr (aimpr, mimpr, and pimpr, respectively; Figs. 2I, 3B). The ilpr is divided into middle ilpr (milpr) and posterior ilpr (pilpr). The distinct structure that protrudes in front of the milpr has been referred to as the optic tubercle (optu) and we followed this convention (Figs. 2F,I, 3B). The lateralmost area of the protocerebrum, which is lateral to the milpr and pilpr, is the lateral horn (LH, Figs. 2E,I, 3B). The border between the LH and the milpr/pilpr is determined by the innervation of the olfactory projection neurons (Tanaka et al., 2004).

The term "lateral protocerebrum" (lpr) is sometimes used to refer to the LH, especially in the studies of olfactory sensory pathways (Stocker et al., 1990). This could be misleading, because the term literally infers the collective area of all the lateral regions of the protocerebrum, which would include not only LH but also slpr, ilpr, etc. (Fig. 3). Thus, we propose that the term LH and lpr should be distinguished explicitly.

The brain region that is ventral to the plane of the MB pedunculus and anterior to the plane of the MB vertical lobe is occupied with the antennal lobe (AL, Fig. 2C,J,K), which is clearly separated from the rest of the central brain by a glial sheath (Fig. 1B). The AL and the antennal mechanosensory and motor center (AMMC), which lies in the ventral posterior area of the AL (Figs. 1A, 2M), are parts of the deutocerebrum (de). The region that is posterior to the great commissure is traditionally called the posterior slope (psl, Fig. 3A). Because psl is a large area that virtually surrounds the esophagus, we divided it into superior psl and inferior psl (spsl and ipsl), which are above and below the esophagus, respectively (Figs. 2C,E, 3B).

We defined the protocerebral area between the AL and spsl as the ventromedial protocerebrum (vmpr, Figs. 2K, 3B). The neuropil structure called the ventral body, or lateral accessory lobe, lies within the vmpr. The area lateral to the vmpr has been referred to as the ventrolateral protocerebrum (vlpr, Figs. 2K, 3B). Glial processes separate most of the border between vmpr and spsl and between vmpr and vlpr. The lateral region behind the great commissure is termed here the posterior lateral protocerebrum (plpr, Figs. 2K, 3B). Note that in some previous studies, the term "psl" may include the region that we distinguished as plpr (Fig. 3A).

The central complex (CC, a combined structure of the protocerebral bridge: pb, fan-shaped body: fb, ellipsoid body: eb, and noduli: no) is embedded at the border between mimpr, pimpr, vmpr, and spsl (Fig. 2A–E,I,J). A prominent glial structure covers the border surrounding the CC.

The brain region below the protocerebrum belongs to the deutocerebrum (de; Fig. 2A,L), which contains the AL and AMMC. The region posterior to the deutocerebrum is occupied by the inferior psl (ipsl, Fig. 2M). The tritocerebrum is not discernible in the adult fly brain. The ventralmost area of the central brain is the subesophageal ganglion (SOG), which is detached from the proto-, deuto-,

and tritocerebra in insects like grasshoppers, but is completely fused in flies. The deutocerebrum and ipsl cover the lateral and lateral-posterior areas of the SOG, respectively (Figs. 2A,L,M, 3B). The SOG can further be divided into three segments: the mandibular, maxillary, and labial neuromeres. The border between these neuromeres is difficult to identify, however.

Canonical naming system of the VPNs

In order to refer to various types of VPNs with self-explanatory names, we employed a two-letter naming system for the VPNs. The first character indicates the neuropil of the optic lobe it innervates: i.e., L (Lobula), P (lobula Plate), M (Medulla), and C (Complex of more than one neuropil). The second character indicates the pattern of arborization in the optic lobe: C (Columnar) and T (Tangential or Tree-type, see below). Neuron types that fall in the same category were distinguished by numbers. To indicate the position of the cell bodies, separate ranges of numbers 1–30, 31–60, and 61–90 are reserved for the VPNs whose cell bodies lie in the lateral cell body region (LCBR, the area between the central brain and the optic lobe, Fig. 1A,B), in the central brain, and in the optic lobe, respectively. For example, the neuron type "LT32" is the second type of the VPN category that arborizes in Lobula, has tangential or tree-type arborization, and has cell bodies in the central brain.

Indicating the position of the cell bodies in each VPN name is important practically because the locations of the cell bodies are often correlated with their developmental origin. VPNs in different species could be determined as identical if they share the same arborization pattern in the optic lobe and the same innervation target and the trajectory of projection in the central brain. The cell body position, however, might be shifted in distant species, sometimes crossing the border between the central brain, lateral cell body region, and the optic lobe. In such an exceptional case, the correlation between the number range and the cell body location may not be maintained.

Using Golgi impregnation, Fischbach and Dittrich (1989) reported seven types of lobula-specific columnar neurons (Lcn1, 2, and 4–8) and 10 types of lobula tangential neurons (Lt1–10). In favor of consistency and simplicity, we removed "n" from the former abbreviation and used only uppercase characters. In the previous study, information about both the arborization pattern in the lobula and the projection target in the brain is provided only for Lcn4, 6, and Lt1, 10. We identified VPNs with the same morphological characteristics with these neurons and assigned the same number to keep compatibility. As for other Lcn and Lt neurons (Lcn1, 2, 5, 7, 8, and Lt2–9), the previous study described only arborization patterns within the lobula, making it difficult to establish an unambiguous comparison between their observation and our results. To avoid confusion, we skipped these numbers when assigning numbers to the VPNs we identified in this study.

Clarification of signals from the identified VPNs

Although we tried to identify the GAL4 enhancer-trap strains that label each type of VPN more specifically, there were no lines that selectively label VPNs without labeling any other cells of the brain (see Ito et al., 2003, for this problem). The VPNs and other labeled cells, therefore, might appear intermingled in the 3D reconstruction, making it very difficult to distinguish the morphology of the labeled VPNs (Fig. 4A). In some strains, different types of VPNs are also labeled simultaneously. To clean up the reconstructed image in these cases, we manually erased signals from the cells other than the identified VPNs from each section of the confocal stack (see Materials and Methods). Although this procedure requires laborious manual work of processing more than 100 photographs per each dataset (typically it took 2–4 days), the resulting reconstruction, which looks like a camera-lucida drawing with stereographic depth information, clearly demonstrates the 3D structure of the labeled cells (Figs. 4B, 7–10; see also Supplemental data).

The resulting clear images, however, might be misleading if these GAL4 strains are to be used for driving ectopic expression of effector genes like toxins and synaptic transmission blockers. In such cases, expression in the cells that are erased from these images might play crucial roles that could affect the phenotype. To provide information for assessing the specificity of the real GAL4 expression pattern, we therefore present the reconstructed images of the original confocal data in Figures 15 and 16.

Determination of neuropil layers and the central brain regions innervated by the VPNs

Previous studies on the local and interneurons that connect within and between optic lobe neuropils suggest that axons of photoreceptors R7 and R8 and those of the lamina interneurons that transmit signals from photoreceptors R1–6 terminate at different layers of the medulla (Fig. 1C). These layers in turn are connected preferentially with different layers of the lobula and lobula plate (Fischbach and Dittrich, 1989). Specific movement of the grating patterns invokes the uptake of $[^3H]_2$-deoxy-D-glucose in distinct layers of the optic lobe neuropils (Buchner et al., 1984; Bausenwein and Fischbach, 1992). Several antibodies, such as those against GABA, GAD, and RDL, label different layers selectively (Buchner et al., 1988; Harrison et al., 1996). These suggest that different layers of each optic lobe neuropil might process different types of visual information. From this point of view it is important to understand the central brain regions that are preferentially associated with a particular lobula layer.

The lobula neuropil has been classified into six layers (Fischbach and Dittrich, 1989). The layer that is topologically closest from the medulla (0% depth) is defined as lobula layer 1 (Lo1), and the layer adjacent to the central brain (100% depth) is termed layer 6 (Lo6, Fig. 4C).

When the confocal micrographs are taken with high sensitivity at the excitation wavelength of 458 nm, autofluorescence of the specimen can be detected. We determined the border of the lobula neuropil using this background signal and measured the depth of the arborizations of the labeled VPNs in the horizontal sections (Fig. 4C). Similarly, the region of the central brain innervated by the identified VPNs was determined by comparing the GFP signal with the landmarks that are visible in the background signal and described according to the canonical naming scheme explained above.

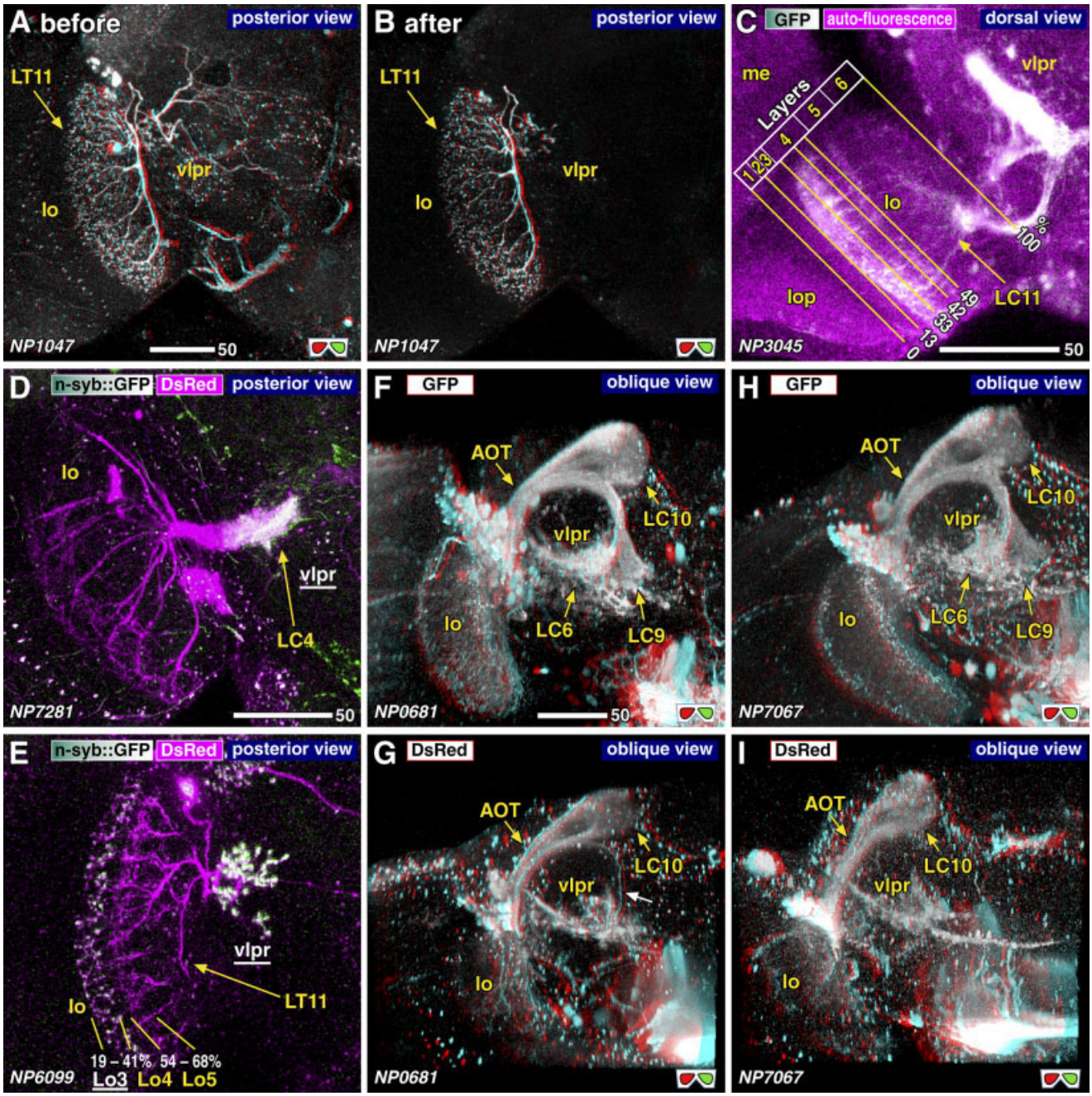

Fig. 4. Techniques used for visualizing the labeled VPNs. **A,B:** 3D reconstruction of the confocal image data before (A) and after (B) signals of other cells than the VPNs are erased manually. The icon of a pair of glasses at the right-bottom corner indicates that the image is a 3D stereogram. Depth information can be obtained when the images are viewed with red filter on the left eye and green or cyan filter on the right eye. Number at the left-bottom corner indicates the GAL4 strain number used for visualizing the neurons. **C:** Visualization of labeled neurons with the unlabeled background structure. Using a confocal microscope, GFP signal (green to white) is excited at 488 nm and recorded with a bandpass filter (500–540 nm). Autofluorescence of the specimen (magenta) is excited at 458 nm and recorded with a long-pass filter (475 nm). As the green signal coincides with the magenta background, it appears white. The medial and lateral border of the lobula is detected in the horizontal section, and the percentage of the depth of the labeled arborization is measured. (In this sample it is 13–33% and 42–49%.) The result is compared with the border between the six layers (0, 10, 16, 23, 52, 75, and 100%, respectively; Fischbach and Dittrich, 1989), and the corresponding layer number is assigned (in this sample, Lo2, 3, and 4 layers). **D,E:** Double staining with the presynaptic site-targeted n-syb::GFP (green to white) and cytoplasmic DsRed (magenta). **F–I:** Difference of the visualized cells depending on the reporter strain. The LC6/9 neurons are visualized with UAS-*GFP* (F,H) but not with UAS-*DsRed* (G,I). Note that *DsRed* visualizes a thin bundle of LC6 axons in NP0681 (white arrow in G) but not in NP7067. Scale bars = 50 μm.

Identification of presynaptic sites

In order to understand the direction of information flow via chemical synapses, it is important to identify the distribution of presynaptic sites (i.e., output synapses) in each identified neuron. Since the age of Ramón y Cajal this was usually attained by presuming the sites of presynapses based on their characteristic morphology. In *Drosophila*, the presynaptic sites of a particular cell can specifically be visualized by the targeted expression of neuronal synaptobrevin (n-syb) fused with GFP (n-syb::GFP) (Ito et al., 1998; Estes et al., 2000). The n-syb, which is an insect homolog of the mammalian vamp, is the protein associated with the docking of synaptic vesicles to the presynaptic membrane, and therefore accumulates in the presynaptic sites.

For the simultaneous visualization of the presynapses and the overall neural morphology, we made a strain that carries both UAS-*n-syb::GFP* and UAS-*DsRed S197Y* (Verkhusha et al., 2001). Using this strain we were able to visualize that the presynaptic sites are distributed in only specific subregions of the arborizations (Fig. 4D,E). In the case of LC4, for example, n-syb::GFP was observed in the vlpr, whereas the extensive branches in the lobula are devoid of presynapses (Fig. 4D). This strongly suggests that LC4 conveys information from the lobula to the central brain (i.e., centripetal pathway). In LT11 neurons, on the other hand, presynaptic sites are observed in the vlpr and in the outer (lateral) layer of the lobula (Lo3 and Lo4 layers), but not in the inner (medial) layer (Lo5; Fig. 4E). It is likely in such a case that visual information is sent from the Lo5 layer centrifugally to Lo3/4 layers and centripetally to the vlpr.

Although different UAS-reporters label the same set of GAL4-expressing cells in most cases, it occurs sometimes that neurons that can be visualized with one UAS-reporter strain would not be visualized if a different reporter strain is used (Ito et al., 2003). This seems to occur in a cell type-specific manner, which is in some cases convenient for limiting the types of the cells visualized. For example, in spite of our extensive screening we could not identify GAL4 strains that can specifically label LC10 neurons. The GAL4 strains used in this study all label LC6, 9, and 10 neurons simultaneously when crossed with the UAS-*GFP* (T2) strain (Fig. 4F,H). When these lines are crossed with the UAS-*DsRed* strain, however, only LC10 neurons are visualized (Fig. 4G,I).

Classification of the arborization patterns in the optic lobe

VPNs can also be categorized into three types according to the characteristic morphology of their arborization in the optic lobe. Each optic lobe neuropil consists of the visual cartridges that correspond to the composition of the ommatidia in the compound eye. The arborizations of the columnar VPNs run parallel to the visual cartridges (Fig. 5A–C). The overall structure of such VPNs appears like a series of columns (Fig. 5B). A single neuron arborizes within one or a few cartridges and therefore covers only a small portion of the visual field (Fig. 5C).

The second type is the tangential VPNs (Fig. 5D–F). Their arborizations spread perpendicular to the cartridges at a specific layer level. A single neuron of this type arborizes across cartridges and therefore covers a large, if not all, area of the visual field (Fig. 5F).

We also identified a variation of tangential VPNs, which we named tree-like VPNs (Fig. 5G,H). Unlike tangential VPNs, the terminal branches of the tree-like VPNs do not run perpendicular to the visual cartridges. Rather, they run parallel to the visual cartridges like that of the columnar VPNs. However, they are similar to the tangential neurons in that a single neuron covers a very large area of the visual field, making horizontal connections among a large number of visual cartridges (Fig. 5H). Therefore, although their structure appears different, the tangential and tree-like VPNs would be similar functionally.

Screening of the GAL4 enhancer-trap strains that label specific types of the VPNs

In the following sections we report the screening and identification of the lobula-specific VPNs. First, we examined the brains of 3,939 GAL4 enhancer-trap strains and identified 274 candidate strains (7% of the screened lines) in which VPNs were labeled relatively specifically. We subjected these lines to detailed serial confocal microscopy and chose 96 strains (2%) that 1) express GAL4 in none or only a few other types of neurons in the optic lobe, and 2) express GAL4 in a relatively small number of other cells in the central brain.

Comparing the staining patterns of these 96 strains, we identified 44 pathways of VPNs. Among them, 14 pathways were associated specifically with the lobula (L: lobula-specific VPNs), 10 pathways specifically with the lobula plate (P: lobula plate-specific VPNs), and 9 pathways specifically with the medulla (M: medulla-specific VPNs). There were also 11 pathways that contribute to a complex of more than one neuropil of the optic lobe (C: complex-type VPNs).

In this study we concentrate on the 14 lobula-specific VPNs (Fig. 6; Table 1). Seven of them are identified unambiguously with the neurons that have been reported previously. Among the 14 pathways of VPNs, 12 have their cell bodies in the lateral cell body region, and only two pathways (one cell for each) have their cell bodies in the central brain. There was no lobula-specific VPNs that have their cell bodies in the outer surface of the optic lobe. The number of the labeled cell bodies was counted in three independent brain samples (Table 2). The total number of the lobula-specific VPNs identified in this study was ~500.

Description of the identified VPNs

In this section we describe the detailed structure of each identified VPN type. Figure 6 and Table 1 summarize the projection pattern. Figures 7–10 show the 3D reconstruction images viewed from three directions. Because lobula lies in the posterior area of the brain, the coronal 3D reconstruction is viewed from the posterior. The trajectory of each VPN pathway in the 3D space can be recognized by comparing the posterior and dorsal views. In addition, the oblique view from the posterior-dorsal direction is presented, because this viewing angle visualizes the layers in the lobula most clearly. Figures 11–13 show the detailed structure of the labeled cells and Figure 14 describes the distribution of presynaptic sites. Figure 17 summarizes the distribution of the cell bodies in the lateral cell body region and the terminal areas in the vlpr. Virtual reality movies of the identified VPNs are available as Supplemental data.

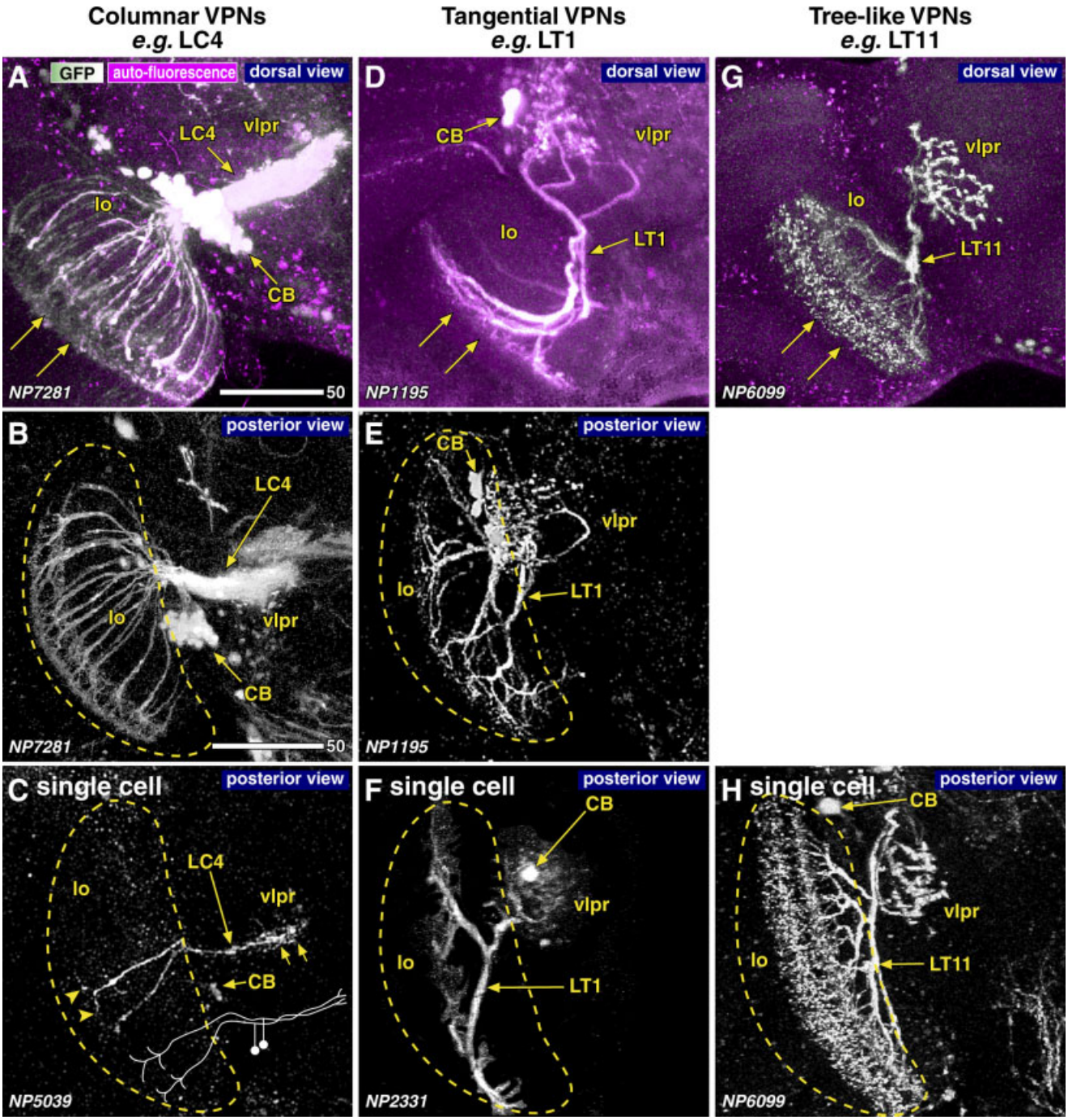

Fig. 5. Three morphological classes of VPNs. Images of columnar (**A–C**), tangential (**D–F**), and tree-like (**G,H**) VPNs. 3D reconstruction of a small number of sections, showing the dorsal (A,D,G) and posterior (B,E) views of multiple neurons and the posterior view of single neurons (C,F,H). A pair of arrows in A,D,G indicate the direction of the visual columns. Dashed lines indicate the contour of the lobula. Drawing in C shows the schematics of the two neurons labeled in this sample. CB, position of the cell bodies. Erased cells: B: CC, CT, PC, and MT; C: thick fibers in the central brain; E: MT, HS, and VS cells; F: PT neurons and one of the two LT1 neurons labeled. Scale bar = 50 μm.

Columnar neurons

We identified eight types of lobula-specific columnar neurons and named them LC4, 6, and 9-14 (Table 1). Numbers 1, 2, 5, 7, and 8 were skipped to avoid confusion with the neurons for which only parts of the innervation patterns in the optic lobe have been described (Fischbach and Dittrich, 1989). Because the same study did not describe Lcn3, we also skipped this number to keep consistency.

LC4. LC4 neurons (Fig. 7A–C) have previously been identified as lobula columnar neurons 4 (Lcn4) (Fischbach

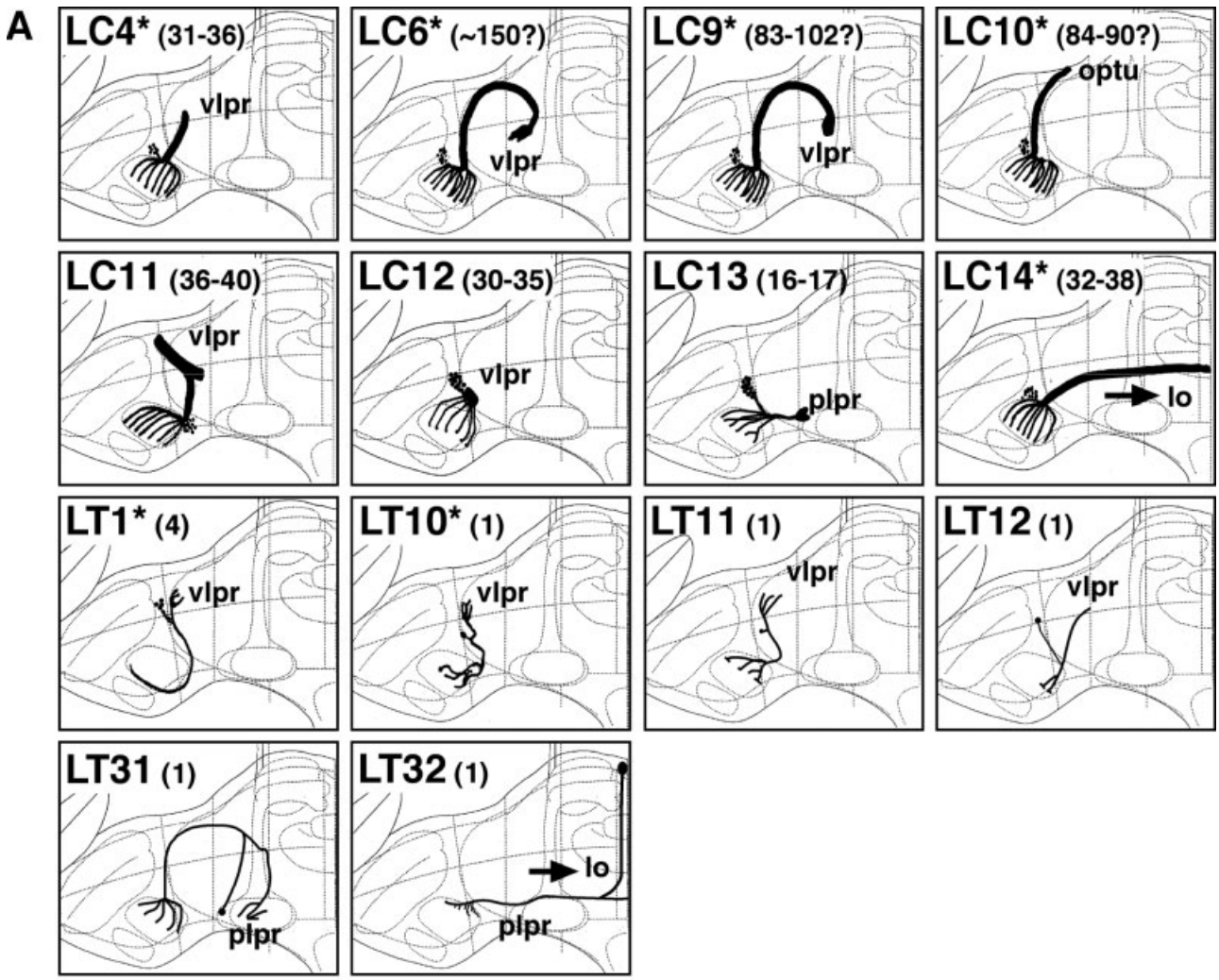
A
LC4* (31-36)
vlpr
LC6* (~150?)
vlpr
LC9* (83-102?)
vlpr
LC10* (84-90?)
optu
LC11 (36-40)
vlpr
LC12 (30-35)
vlpr
LC13 (16-17)
plpr
LC14* (32-38)
lo
LT1* (4)
vlpr
LT10* (1)
vlpr
LT11 (1)
vlpr
LT12 (1)
vlpr
LT31 (1)
plpr
LT32 (1)
lo
plpr

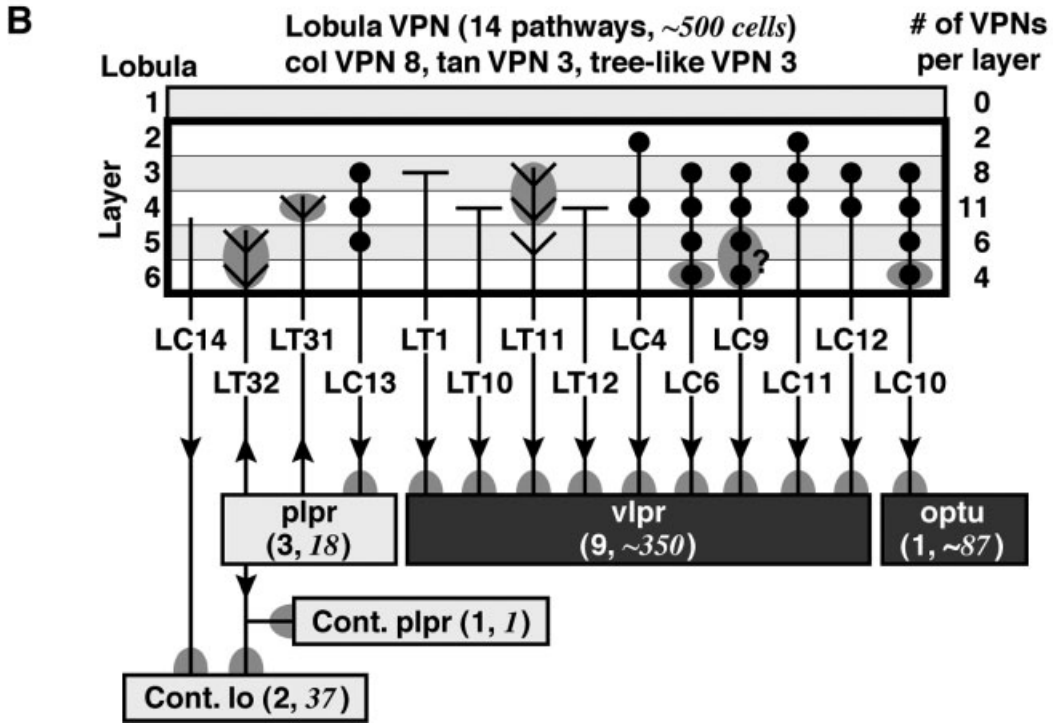
B
Lobula VPN (14 pathways, ~500 cells)
col VPN 8, tan VPN 3, tree-like VPN 3
# of VPNs per layer
Lobula
Layer
1
2
3
4
5
6
0
2
8
11
6
4
?
LC14
LT32
LT31
LC13
LT1
LT10
LT11
LT12
LC4
LC6
LC9
LC11
LC12
LC10
plpr (3, 18)
vlpr (9, ~350)
optu (1, ~87)
Cont. plpr (1, 1)
Cont. lo (2, 37)

Figure 6

and Dittrich, 1989). In all, 25–29 cell bodies (CB) were observed in the mid-ventral area of the lateral cell body region and 6–7 cells were located in its anterior area (Fig. 17A). The cell body fibers (cbf), with which we refer to the region of the neural fibers between the cell body and the first point of branching or arborization, form a bundle that runs toward the "neck" of the lobula, which is the medial edge of this neuropil where all the lobula-specific VPNs converge (Fig. 7A). At the neck, the fibers bifurcate to contribute to the lobula and to the vlpr. In the lobula they form clear columnar projections that cover the whole visual field (Figs. 5B, 7A, 11A–C). Whereas the medial half of the lobula contains only thick branches, the lateral half is rich in numerous fine arborizations, with bistratified varicosities in layers Lo2 and Lo4 (Figs. 7B, 11C).

In the central brain, the fibers form a thick prominent bundle ("lobula/lobula plate bundle") (Fischbach and Dittrich, 1989; Strausfeld and Gilbert, 1992; Douglass and Strausfeld, 2003), which terminates in the posteriormost medial area of the vlpr (Fig. 11B,C). These terminals form a blunt, stick-like ending. Single neurons of this pathway send fibers along the visual cartridges. Figure 5C shows two such VPNs that arborize in different visual cartridges. Detailed examination of confocal sections revealed that the two axons intertwine as they project to the vlpr but eventually arborize in a separate area of the vlpr (schematic drawing in Fig. 5C). This would suggest that some sort of retinotopic spatial map is maintained between the lobula and the vlpr.

The n-syb::GFP labeling was observed only in the medial half of the stick-like ending in the vlpr (Fig. 4D). Single-neuron staining clearly shows varicosities in this area (arrows in Fig. 5C). LC4 is therefore centripetal (Fig. 6B). Branches in the lobula, which are not labeled with n-syb::GFP, also show varicosity-like structures (arrowheads in Fig. 5C), although the size of these blebs is relatively small.

LC6. LC6, 9, and 10 are neurons that form the anterior optic tract (AOT; Power, 1943), a prominent fiber bundle that runs from the lobula to the optic tubercle (optu, Fig. 2H–J). The cell bodies of these neurons form a single large cluster in the mid dorsal area of the lateral cell body region (Fig. 17A). Like all other LCs, the cell body fibers run towards the lobula neck and bifurcate there (Fig. 7D,G,J). Whereas LC6 and 9 make a round turn in the midway of the AOT to terminate in the vlpr (Fig. 7D–I), LC10 projects to the optu (Fig. 7J–L). The bundles of LC6/9 and LC10 are separated clearly in the AOT (Figs. 4F,H, 12A). The semicircular trajectory in the vlpr is characteristic of LC6/9. They are also the only VPNs that enter the vlpr from its anterior side (Fig. 17B,C).

Neurons in the AOT have been classified into four types: S1–S4 (Fischbach and Lyly-Hünerberg, 1983). S1 neurons connect different regions of the central brain, but the origin and the projection target of S2 neurons are not described in enough detail. The relatively straight trajectory of the S3 neurons and the round trajectory of the S4 axons indicate that they correspond to the LC10 and LC6/9 pathways, respectively.

The bundles of LC6 and LC9 run together along the AOT. Their trajectories separate only after they enter the vlpr (Fig. 12A,C). LC6 forms a steeper turn than LC9 and terminate in the lateralmost area of the dorsal posterior vlpr (Figs. 12D, 17B,C). The distal end of the bundle spreads horizontally to form a triangular shape that spans from the central vlpr to its lateral edge (arrowheads in Figs. 7D–F, 12D). Golgi impregnation study identified the LC6 neurons as Lcn6, which arborize in the Lo3, 4, and 5 layers (Fischbach and Dittrich, 1989). Our study suggests, however, that they also arborize in the Lo6 layer (Figs. 7E, 14A).

The n-syb::GFP signal in the lobula was observed in a thin layer in Lo6 (Fig. 14A). In the vlpr, the output sites are confined in the triangular area. LC6 is therefore a centripetal pathway sending information from Lo3-5 layers to the vlpr, with collateral output to the Lo6 layer (Fig. 6B).

We found no GAL4 strains that specifically label the LC6 neurons. LC6, 9, and 10 neurons are labeled collectively with the NP0681 and NP7067 strains. NP2620, on the other hand, label LC4, 6, and 14. The total cell count in the cluster of the LC6, 9, and 10 neurons was 321–358 (average 333, Table 2). The numbers of the LC9 and LC10 neurons were likely to be slightly less than 83–102 (average 94) and 84–90 (average 87), respectively (see below). The difference, on average slightly more than 152 cells, could be attributed to the LC6 neurons. The number of the LC6 neurons can also be estimated in another way. The strain NP6250 labels LC9 and 10 neurons strongly but LC6 only faintly. If we assume that most of the cells counted in this strain (151–216, average 190, Table 2) belongs to LC9 and 10, the difference between this cell count and the total cell count of the LC6, 9, and 10 neurons, i.e., slightly more than 143 on average, could be attributed to the LC6 neurons. Thus, two lines of evidence suggest that the cell number of the LC6 would be around 150 (Table 1).

LC9. Like LC6, the cell bodies of the LC9 neurons lie in the mid dorsal area of the lateral cell body region (Fig. 17A). In the lobula they are likely to arborize in the Lo3, 4, 5, and 6 layers, forming two layers of densely contributed areas in Lo3/4 and Lo5/6 (Figs. 7H, 12B). The bundles of LC9 axons run separately from that of the LC10 neurons (Fig. 12A). The bundle makes a round turn shortly after the AOT reaches the lateralmost area of the optu (optu3, see next section, Fig. 12A). After entering the vlpr, the LC9 axons run straight posteriorly to terminate in the central part of the dorsal posterior vlpr (Figs. 4F,H, 7G–I, 12A, 17B,C). The terminal area of the LC9 spreads to form a triangular shape with two apices in its lateral and medial sides (arrowheads in Figs. 7G–I, 12E).

Fig. 6. Summary of the identified VPNs. **A:** Schematic drawing of the projection pattern of each identified VPN pathway, shown in dorsal view. Small circles represent the positions of the cell bodies. Numbers in parentheses indicate the cell count of the labeled VPNs per pathway. Those with question marks are estimated numbers. Asterisks indicate the pathways reported previously. **B:** Distribution of arborizations and presynaptic sites. Black circles, horizontal lines, and hooked lines represent the columnar, tangential, and tree-like arborizations, respectively. Gray circles indicate the presynaptic sites. Question mark in LC9 indicates that the existence of the presynapses is not completely confirmed (see Fig. 14B). Arrows show the deduced direction of information. Numbers in parentheses indicate the number of the identified pathways and VPN cell numbers (in italics) innervating the respective neuropils. Cont. indicates the neuropil in the contralateral hemisphere.

TABLE 1. List of the Identified VPNs

VPN name	Previous reports	Cell count	Arborization	Direction	Layers	Central brain	Laterality	Cell body	Presynapses
LC1	Lcn1 (1)	—							
LC2	Lcn2 (1)	—							
LC4	Lcn4 (1)	31–36	columnar	centripetal	Lo2, 4	vlpr	ipsi	LCBR	vlpr
LC5	Lcn5 (1)	—							
LC6	AOT (4) Lcn6 (1) S4 (1, 2)	~150?	columnar	centripetal	Lo3, 4, 5, 6	vlpr	ipsi	LCBR	Lo6, vlpr
LC7	Lcn7 (1)	—							
LC8	Lcn8 (1)	—							
LC9	AOT (4)	83–102?	columnar	centripetal	*same as LC6?*	vlpr	ipsi	LCBR	Lo5, 6?, vlpr
LC10	AOT (4) S3 (1, 2) LCN (3)	84–90?	columnar	centripetal	*same as LC6?*	optu	ipsi	LCBR	Lo6, optu
LC11	—	36–40	columnar	centripetal	Lo2, 3, 4	vlpr	ipsi	LCBR	vlpr
LC12	—	30–35	columnar	centripetal	Lo3, 4	vlpr	ipsi	LCBR	vlpr
LC13	—	16–17	columnar	centripetal	Lo3, 4, 5 ventral	plpr	ipsi	LCBR	plpr
LC14	Cco (4) GC (3) atoGAL4 (5)	32–38	columnar	contra	Lo surface	contra-lo	interOL	LCBR	lo surface
LT1	Lt1 (1)	4	tangential	centripetal	Lo3	vlpr	ipsi	LCBR	vlpr
LT2	Lt2 (1)	—							
LT3	Lt3 (1)	—							
LT4	Lt4 (1)	—							
LT5	Lt5 (1)	—							
LT6	Lt6 (1)	—							
LT7	Lt7 (1)	—							
LT8	Lt8 (1)	—							
LT9	Lt9 (1)	—							
LT10	Lt10 (1)	1	tangential	centripetal	Lo4 dorsal	vlpr	ipsi	LCBR	vlpr
LT11	—	1	tree-like	centrifugal + centripetal	Lo3, 4, 5	vlpr	ipsi	LCBR	Lo3, 4, vlpr
LT12	—	1	tangential	centripetal	Lo4 posterior	vlpr	ipsi	LCBR	vlpr
LT31	—	1	tree-like	centrifugal	Lo4	plpr	ipsi	brain (near plpr)	Lo4
LT32	—	1	tree-like	centrifugal	Lo5, 6	contra-lo, plpr	interOL	brain (oesophagus)	Lo5, 6, contra-plpr
total		ca. 500							

See Figures 1 and 2 for abbreviations of the brain regions. Minimum and maximum numbers of the observed cell counts are shown. For LC6, 9, and 10, cell numbers are estimated as explained in the text, contra, contralateral; ipsi, ipsilateral; interOL, interconnecting corresponding optic lobe neuropiles. Reference: (1) Fischbach and Dittrich, 1989; (2) Fischbach and Lyly-Hünerberg, 1983; (3) Fischbach, 1983; (4) Power, 1943; (5) Morales et al., 2002.

The n-syb::GFP signal in the lobula was observed in broader layers than LC6. It is rather likely that the presynaptic sites would be distributed both in Lo5 and Lo6 layers. In the vlpr, presynaptic sites are confined in the posteriormost end of the bundle (Fig. 14B). Thus, LC9 is a centripetal pathway with the collateral output in the Lo5 and 6 layers (Fig. 6B). It is important to note that, although LC6 and LC9 run through the anterior vlpr, they form presynapses only in the posterior area of the vlpr (Fig. 17B). It is likely that the anterior part of the vlpr does not receive visual information.

Like LC6, none of the GAL4 strains label LC9 specifically. The strain NP6563 is most specific, which labels some of the LC10 neurons only faintly. If we assume that most of the cells labeled in this strain would be associated with LC9, the cell count would be slightly less than 83–102 (Tables 1, 2).

LC10. Among the three LC types that comprise the AOT, LC10 is the only pathway that projects to the optic tubercle (Fig. 7J–L). It has previously been identified as S3 (Fischbach and Lyly-Hünerberg, 1983; Fischbach and Dittrich, 1989) and LCN (Fischbach, 1983). In the lobula, LC10 neurons arborize in Lo3, 4, 5, and 6 layers (Fig. 7K). In most of the samples we examined the distal (medial) end of the AOT thickens to form a cone-like structure of the optu (Figs. 7J, 12G). Extensive terminal arborization is observed in this region.

The optu can be divided into three regions according to the density of the arborizations (Fig. 12G,H). The medialmost (optu1) and lateralmost (optu3) regions contain dense arborizations of the LC10 neurons. The area in between (optu2) is essentially devoid of LC terminals. High-magnification reconstruction of this area suggests that there are three different types of fibers (Fig. 12H). It is likely that the LC10 neurons can be classified into three subtypes, which we termed LC10A, B, and C. Although we could not isolate the GAL4 strains that label each subset of the LC10 neurons, in one of the three DsRed samples we found that GAL4 accidentally failed to drive the DsRed expression in LC10B and C neurons, visualizing clearly the trajectory of the LC10A neurons (Fig. 12F,J–L). The axons of the LC10A neurons run through the ventral area of the optu to circumvent optu2 (Fig. 12H,J,K). Upon reaching optu1, they project dorsally and terminate in the anterior area of the optu1 (Fig. 12J–L). LC10B axons run in the dorsal region of the optu, project straight through optu2, and terminate in the posterior dorsal area of optu1 (Fig. 12H,I). LC10C axons are shorter and terminate in optu3 (Fig. 12H).

In the optic lobe, n-syb::GFP signal is observed in the Lo6 layer (Fig. 14C). The varicosities in the Lo3–5 layers are devoid of presynapses and are hence likely to be postsynaptic. In the optu, presynaptic sites are distributed throughout optu1 and at the medial end of optu3 (Fig. 14C). Taken together, it is likely that LC10 neurons form a centripetal pathway that collects information from Lo3–5 layers and transmit the signal first to Lo6 and then to optu1 and optu3 (Fig. 6B).

Although none of the GAL4 strains labeled LC10 specifically when UAS-*GFP* was used as reporter, the combination of the NP0681 and NP7067 strains with the UAS-*DsRed* strain visualized LC10 neurons specifically (Fig.

TABLE 2. List of the GAL4 Enhancer-Trap Strains

VPN name	GAL4 strain	Cell count min	Cell count mid	Cell count max	Label in the optic lobe	Difference with DsRed	Locus, chromosome	Related genes (GETDB data)
LC4	NP7281		31		LC4, CC, CT, PC, MT	not CC	?, 1st	—
	NP7476*	31	33	36	LC4, medulla intrinsic	same	93C4, 3rd	SNF4Agamma, CG7000
	NP7365		n.d.		LC4, LT12, PT, MT	same	?, 2nd	CG40262, CG40264
	NP5039	2	6	8	LC4 (a few cells)	n.d.	4D7, 1st	Ptp4E, CG4068
	NP2620		n.d.		LC4, LC6, LC14, MT, PC	LC14 stronger	22A6, 2nd	jockey{}288, CG31666
LC6	NP2620		n.d.			LC4, LC6, LC14, MT, PC	*see above*	*see above*
	NP0681	321	330 (with GFP)		LC6, 9, 10, LT1, MT, unidentifiable LT	not LC9 only a few LC6	37B1, 2nd	BEST:LD25345, CG17323, BEST: GH06505
	NP6250		faint		LC6 (faint), LC9, 10, LT1, MT, unidentifiable LT	not LC6, 9	37B1, 2nd	BEST:LD25345, CG17323, BEST: GH06505
	NP7067*	321	335	358	LC6, 9, 10, LT1, MT, unidentifiable LT	not LC6, 9	37B1, 2nd	BEST:LD25345, CG17323, BEST: GH06505
LC9	NP0681		*see above*		LC6, 9, 10, LT1, MT, unidentifiable LT	*see above*	*see above*	*see above*
	NP6250	151	204	216	LC6 (faint), LC9, 10, LT1, MT, unidentifiable LT	*see above*	*see above*	*see above*
	NP7067		*see above*		LC6, 9, 10, LT1, MT, unidentifiable LT	*see above*	*see above*	*see above*
	NP6563*	83	97	102	LC9, LC10 (faint), unidentifiable LT, PT, Y cell (from me to lo/lop)	same	79E3, 3rd	Ten-m, CG14460, CG32450
LC10	NP0681*	84	90 (with DsRed)		LC6, 9, 10, LT1, MT, unidentifiable LT	*see above*	*see above*	*see above*
	NP6250		*see above*		LC6 (faint), LC9, 10, LT1, MT, unidentifiable LT	*see above*	*see above*	*see above*
	NP7067		*see above*		LC6, 9, 10, LT1, MT, unidentifiable LT	*see above*	*see above*	*see above*
	NP6563		faint		LC9, LC10 (faint), unidentifiable LT, PT, Y cell (from me to lo/lop)	*see above*	*see above*	*see above*
LC11	NP3045*	36	39	40	LC11	n.d.	58A2, 2nd	CG13492, CG4363
	NP7226	42	43	47	LC11, VLPRI11	same	19F1, 1st	CG1501, CG15445, CG32516
LC12	NP7302*	30	31	35	LC12, LT31, PT	not c op fo LC12 stronger	?	—
LC13	NP6502*	16	16	17	LC13, MT, medulla interneuron to lo	MT weaker	77E3, 3rd	kni, CG13253
LC14	NP1011		22		LC14	n.d.	?, 1st	—
	NP1320	30		35	LC14, MT	+LC14 variant to me (same as in NP6558)	61F6, 3rd	Myo61F, CG9153
	NP2620		n.d.		LC4, LC6, LC14, MT, PC	*see above*	*see above*	*see above*
	NP6558*	32	37	38	LC14, a variant of LC14 neurons that arborize also in the medulla, lobula plate intrinsic (amacrine)	n.d.	84F6, 3rd	ato, CG11671, CG9630
LT1	NP1195*	4	4	4	LT1, MT, HS, VS	lethal	42C1, 2nd	jing, CG15233, CG15234
	NP2331	2	2	2	LT1, PT	n.d.	85D1, 3rd	D1, pum
LT10	NP1035	1	1	1	LT10, 11	n.d.	13F1, 1st	sd, Chc, CG8509
	NP5006*	1	1	1	LT10	same	?, 1st	—
	NP7121	1	1	1	LT10, unidentifiable LT, MT, glia	same	19E7, 1st	Quasimodo{}189, 1360{}190, Rt1c{}191
LT11	NP1035	1	1	1	LT10, 11	*see above*	*see above*	*see above*
	NP1047	1	1	1	LT11	not LT11	?, 1st	—
	NP6099*	1	1	1	LT11	same	17A4, 1st	CG15061, CG5963
LT12	NP7233	1	1	1	LT12, CT, MT	same	?, 1st	—
	NP7365*	1	1	1	LC4, LT12, PT, MT	*see above*	*see above*	*see above*
LT31	NP7302*	1	1	1	LC12, LT31, PT	*see above*	?	*see above*
LT32	NP2450*	1	1	1	LT32, MT	same	39E1, 2nd	CG31611, CG31613, CG31618, CR31614
total		475	500	533				

Strains that are used for estimating the cell numbers shown in Table 1 are indicated with asterisks. Cells were counted in three individuals whenever possible. "Faint" indicates that the strain labels that cell type only faintly. The "difference with DsRed" field describes the difference between the visualization with UAS-*GFP (T2)* and UAS-*DsRed* reporter strains. For example, "not LC6, 9" means that LC6 and 9 neurons were not visualized when *DsRed* was used as reporter. Locus, chromosome, and related genes (genes near the insertion site) derive from the GETDB database. Question marks in the locus field indicate that the exact insertion points have not been determined. Unidentifiable LT, lobula-specific tangential VPNs whose precise projection pattern could not be identified precisely; MT, medulla-specific tangential VPNs; PC, lobula plate-specific columnar VPNs; PT, lobula plate-specific tangential VPNs; CC, complex- type columnar VPNs; CT, complex-type tangential VPNs; HS, "horizontal system" cells in the lobula plate; VS, "vertical system" cells in the lobula plate; c op fo, commissure of the optic foci.

4G,I). The number of cells the LC10 neurons visualized in this way was 84–90 (Table 2).

LC11. LC11 neurons have their cell bodies in the posterior dorsal area of the lateral cell body region (Figs. 8A–C, 17A). We identified 36–40 cells of this category. The cell body fibers run toward the lobula neck and bifurcate there. Projections to the lobula are columnar and form varicosities in two layers. The lateral arborization occurs in the Lo2, 3, and the lateral area of the Lo4 layer, whereas the medial arborization is observed in the medial area of the Lo4 layer (Figs. 4C, 11F). The LC11 neurons collectively cover all the visual field.

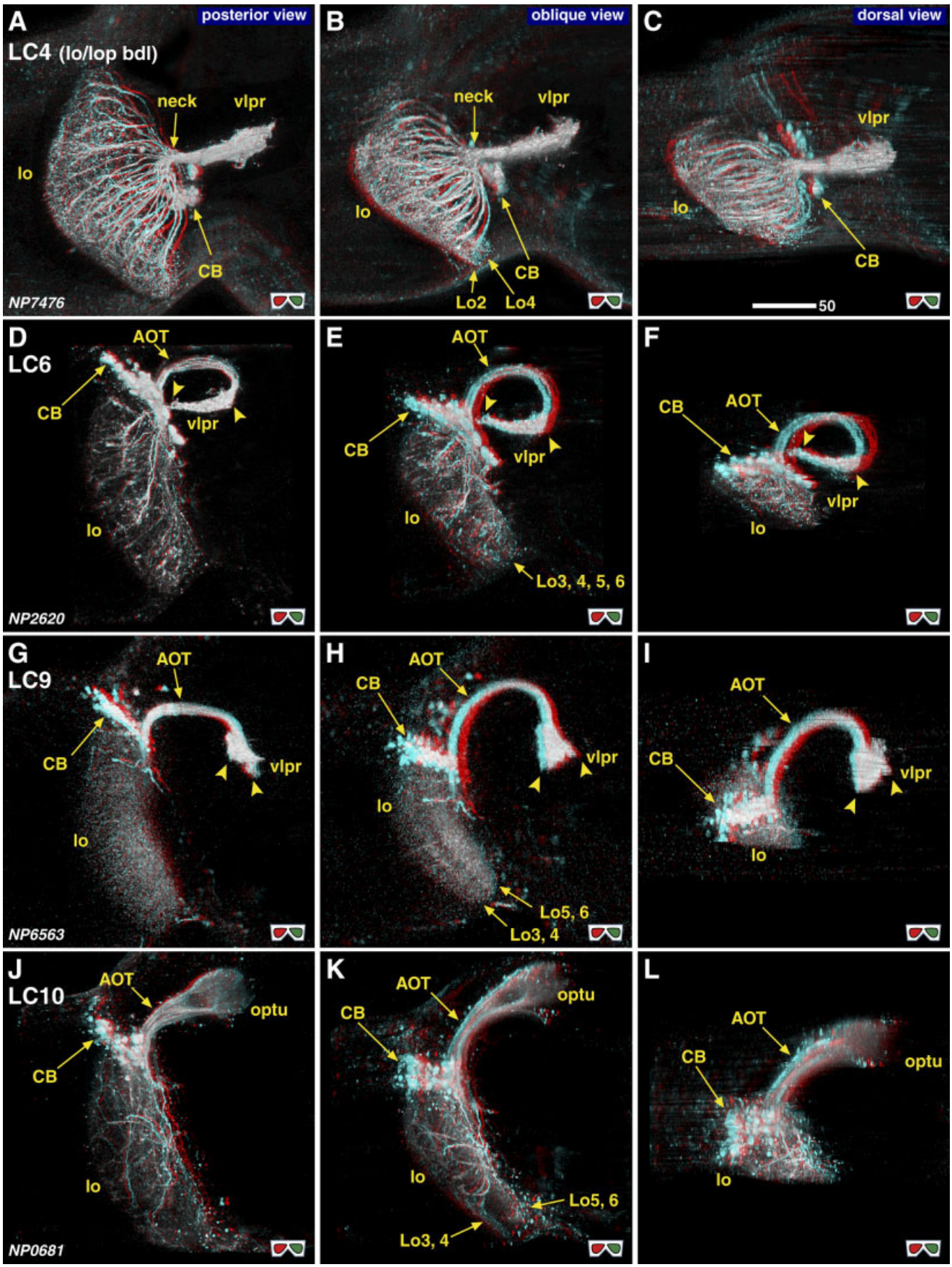
A
posterior view
LC4 (lo/lop bdl)
neck
vlpr
lo
CB
NP7476
B
oblique view
neck
vlpr
lo
CB
Lo2
Lo4
C
dorsal view
vlpr
lo
CB
50
D
LC6
AOT
CB
vlpr
lo
NP2620
E
AOT
CB
vlpr
lo
Lo3, 4, 5, 6
F
CB
AOT
vlpr
lo
G
LC9
AOT
CB
vlpr
lo
NP6563
H
AOT
CB
vlpr
lo
Lo5, 6
Lo3, 4
I
AOT
CB
vlpr
lo
J
LC10
AOT
optu
CB
lo
NP0681
K
AOT
optu
CB
lo
Lo5, 6
Lo3, 4
L
AOT
CB
optu
lo

Figure 7

The fibers form a thin, tightly packed bundle at the lobula neck and enter the plpr (Fig. 11D). The bundle makes a round turn toward the anterior, without arborization, and enters the vlpr from its posterior border. There the bundle becomes thicker and makes a steep turn laterally to form a stick-like structure (white arrows in Figs. 8A–C, 11D–F), which runs anterior-laterally and forms a blunt end in the posterior lateral vlpr (Fig. 11F).

The strain NP3045 labels only LC11 neurons. NP7226, on the other hand, labels additional cell cluster of about 15 cells near the LC11 cell bodies. These neurons do not arborize in the optic lobe and project directly to the vlpr (vlpr intrinsic 11: VLPRI11 neurons). They also form a stick-like bundle that runs parallel to the "stick" component of the LC11 terminals (Figs. 11E, 14D,E). Unlike LC11, the VLPRI11 neurons form extensive branches that fan out above and below the stick and also in the anterior lateral vlpr ("f" in Figs. 11E, 14E).

The labeling of the n-syb::GFP in the LC11 neurons was observed not in the lobula but only in the "stick" component in the vlpr (Fig. 14D,E). The n-syb::GFP signals are densely packed in the whole cross section of the stick. The LC11 neurons are therefore centripetal, sending information from the lobula to the vlpr (Fig. 6B). On the other hand, the stick component of the VLPR11 neurons is devoid of the n-syb::GFP signal. Presynaptic sites are distributed only in the extensive fan-like branches.

Both LC4 and LC11 have extensive columnar arborizations in the lobula. Their varicosities overlap in Lo2 and Lo4 layers (Fig. 6B). Yet their projection targets in the vlpr are strikingly different. Terminals of LC11 are located relatively dorsally, whereas LC4 terminate more ventrally (compare Fig. 11B,E). LC4 enters the vlpr from its lateral side and terminates in the posteriormost area (Fig. 11C). LC11, on the other hand, enters the vlpr from the posterior side and arborizes in the lateral and anterior areas (Fig. 11F). These suggest that an apparently similar set of information from the lobula is conveyed to different subregions of the vlpr (Fig. 17B,C).

LC12. LC12 VPNs project to the lateralmost area of the vlpr (Fig. 8D–F). We found 30–35 cell bodies located in the anterior ventral area of the lateral cell body region (Fig. 17A). The cell body fibers run toward the lobula neck and bifurcate there to contribute to the lobula and to the vlpr. The arborizations in the lobula are thin and columnar.

Synaptic varicosities are observed only in the Lo3 and 4 layers (Fig. 8D). Arborizations from different cells collectively cover all the visual field. At the neck of the lobula, the fibers converge to form a bundle, which projects to the vlpr. Upon entering the central brain, the bundle spreads to form the terminal arborization that has a spherical shape with a diameter of ~15 μm (Fig. 14F). The fibers of the LC12 are very short; the length of the fibers between the lobula and the projection target in the vlpr is only ~13 μm, which is the shortest among the 14 lobula-specific VPNs we analyzed. Presynaptic sites are localized only in the vlpr (Fig. 14F). Thus, it is likely that LC12 cells are centripetal neurons (Fig. 6B), which send visual information unidirectionally from the lobula layer Lo3/4 to the lateralmost area of the vlpr (Fig. 17B,C).

LC13. LC13 (Fig. 8G–I) is the only lobula-specific columnar (LC) pathway that terminates in the plpr. We found 16–17 cell bodies that lie in the anterior ventral area of the lateral cell body region (Fig. 17A). The cell body fibers run dorsally and then bifurcate to contribute to lobula and plpr at the neck of the lobula (Fig. 8G,H). The LC13 neurons have synaptic varicosities in the Lo3, 4, and 5 layers.

Unlike other LC neurons, LC13 neurons arborize only in the ventralmost area of the lobula (Figs. 8G, 11G), where they form columnar projection running parallel along the visual cartridges. The projections from these ventral cartridges form a bundle that runs dorsally towards the lobula neck, where they form a steep turn (Fig. 11G). The bundle turns medially and posteriorly at the lobula neck (Fig. 8G,H), enters the lateral area of the plpr, and forms a cone-like terminal arborization. Presynaptic sites are observed only in the terminal end in the plpr (Fig. 14G). LC13 is therefore centripetal (Fig. 6B).

LC14. The great commissure (GC) is a thick bundle of neural fibers that connect lobulae on both sides of the brain. It was initially described by Power (1943, 1946) as Cco (central commissure). The LC14 neurons project along this tract (Fig. 8J–L). They were also visualized by Fischbach (1983) using Golgi impregnation and by Morales et al. (2002) as atonal-GAL4 expressing cells using the *atoGAL4-14A* strain. We identified 32–38 cell bodies in the mid-dorsal area of the lateral cell body region (Fig. 17A). Like other LC neurons, the cell body fibers run toward the neck of the lobula (Fig. 8J). Unlike other LCs, however, the projections of the LC14 neurons are limited only near the surface of the lobula (Fig. 11H,I). Although the fibers appear columnar, they do not enter the lobula neuropil at any layer. Thus, the LC14 neurons cover only the peripheral area of the visual field.

LC14 neurons are also unique in that they probably have no synapses within the central brain. The n-syb::GFP signal is observed in the lobula but not in the great commissure (Fig. 14H). Interestingly, a subset of arborizations in the lobula is devoid of presynapses. Considering that unidirectional centripetal neurons such as LC4 and LC11–13 have no presynapses in the lobula, it is probable that each LC14 neuron is also unidirectional, sending information from one lobula to the other. The branches that are not labeled with n-syb::GFP are therefore likely to be the dendritic arborizations.

Among the four GAL4 strains we identified, NP6558 has its GAL4 insertion site in the locus of the *atonal* gene, and it is likely that the strain reflects its expression pattern (Morales et al., 2002). In addition to the LC14, NP6558

Fig. 7. Columnar lobula-specific VPNs with the cell bodies in the lateral cell body region. 3D stereograms from posterior (**A,D,G,J**), oblique (**B,E,H,K**), and dorsal (**C,F,I,L**) viewing angles. Arrowheads in D–I indicate the edges of the terminal arborization. CB, cell bodies; cbf, cell body fibers; neck, medial edge of the lobula where all the lobula-specific VPNs converge; lo, lobula; Lo2-6; layers of the lobula, vlpr, ventrolateral protocerebrum; AOT, anterior optic tract; optu, optic tubercle. In D–F and J–L, UAS-*DsRed* was used as the reporter to visualize LC6 and LC10 neurons preferentially. Types of other labeled cells erased from the images are: A–C: medulla intrinsic neurons; D–F: LC4, LC14, MT, and PC VPNs; G–I: faint signal of LC10, PT, and unidentifiable LT, Y cell: J–L, a few LC6 cells (see Table 2). Signals of other neurons that remain in the image of the lobula because their fibers are intermingled with the VPNs of interest and therefore could not be erased: D–F: LC4 and LC14; G–I: Y cells and unidentifiable LT; J–L: a few LC6 cells, LT1 and unidentifiable LT. Scale bar = 50 μm.

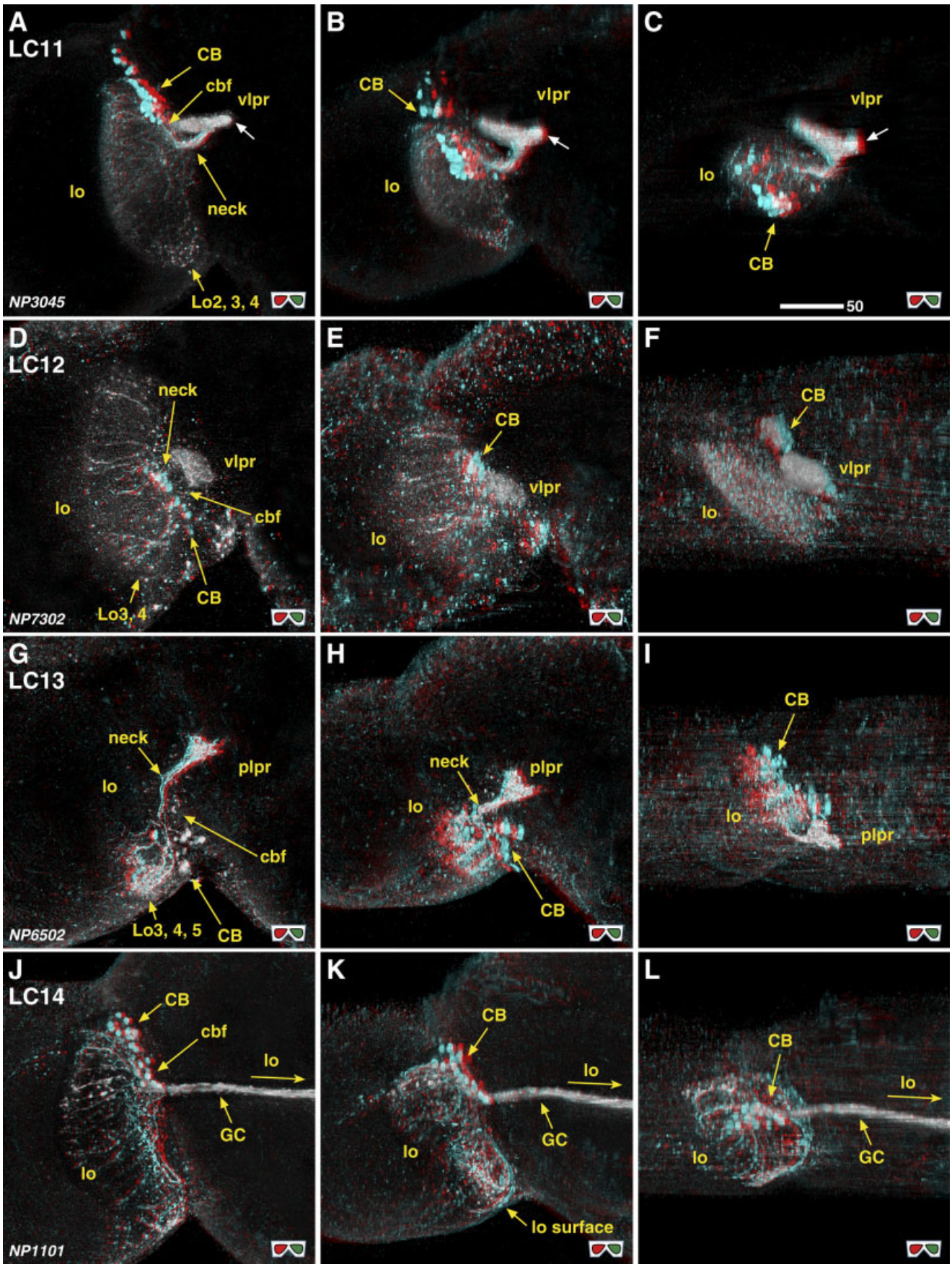

Fig. 8. Columnar lobula-specific VPNs with the cell bodies in the lateral cell body region. 3D stereograms from posterior (**A,D,G,J**), oblique (**B,E,H,K**), and dorsal (**C,F,I,L**) viewing angles. White arrows in A–C indicate the points where VPN bundle makes a round turn. GC, great commissure. UAS-*DsRed* was used in D–F. Erased cells: D–F, LT31 and PT; G–I: MT and medulla interneurons projecting to lobula. Scale bar = 50 μm.

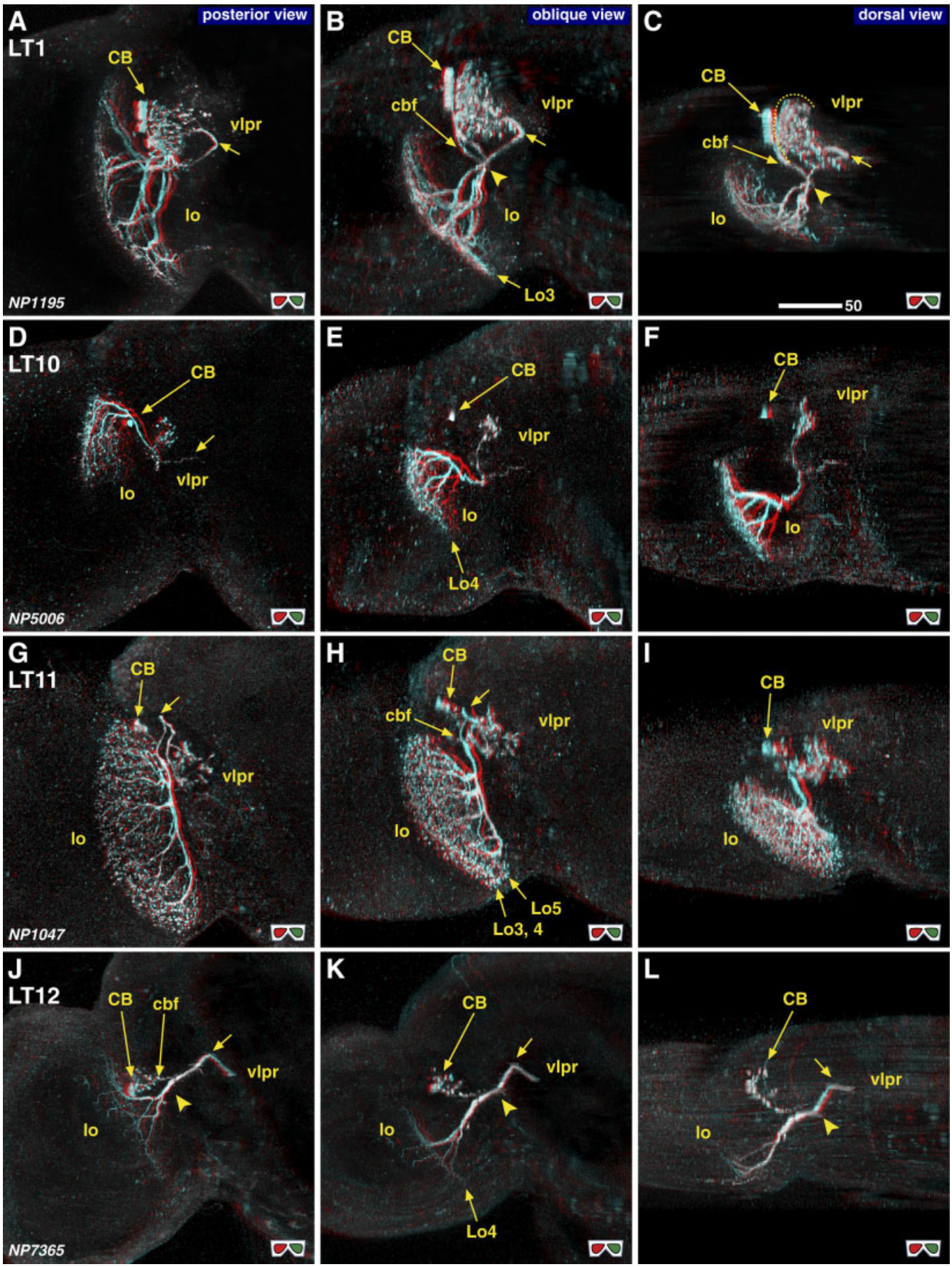

Fig. 9. Tangential and tree-like lobula-specific VPNs with the cell bodies in the lateral cell body region. 3D stereograms from posterior (**A,D,G,J**), oblique (**B,E,H,K**), and dorsal (**C,F,I,L**) viewing angles. Arrows in A–C,G,H,J–L indicate the points where fibers make a steep turn. Arrow in D indicates a thin collateral. Arrowheads indicate the bifurcation point of the cbfs. Erased cells: A–C: MT, HS, and VS; J–L: LC4, PT, and MT. Scale bar = 50 μm.

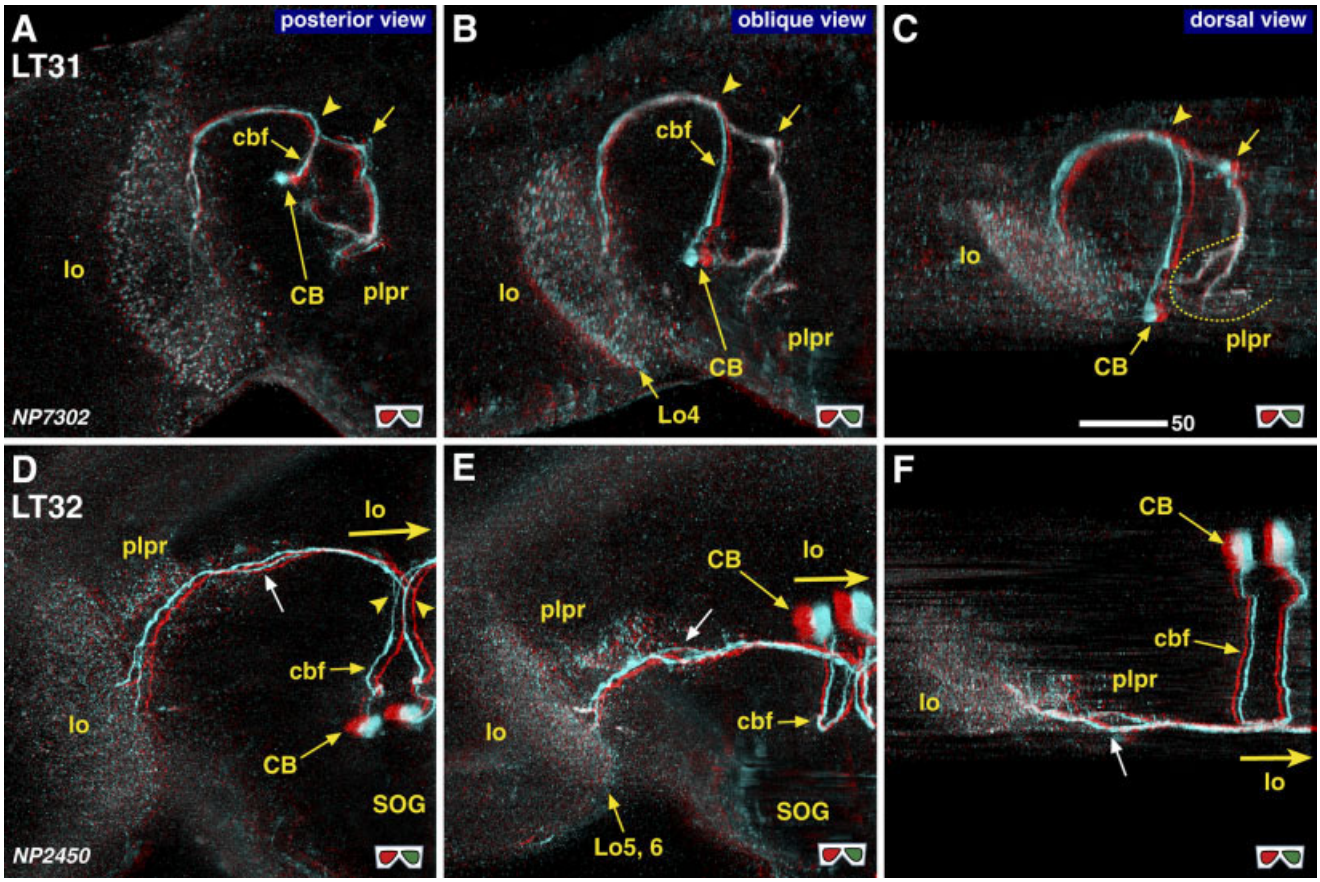

Fig. 10. Tree-like lobula-specific VPNs with the cell bodies in the central brain. 3D stereograms from posterior (**A,D**), oblique (**B,E**), and dorsal (**C,F**) viewing angles. Arrowheads indicate the bifurcation point of the cbfs. Arrows in A–C indicate the point where the fibers make a right-angled turn. White arrows in D–F indicate the collateral fiber branches innervating the plpr. Erased cells: A–C: LC12 and PT; D–F: MT. Scale bars = 50 μm.

labels intrinsic neurons in the lobula plate as well as a variant of the LC14 neurons that send thin projections to the medulla, which may connect the medulla in each side of the brain (Fig. 16C).

Tangential or tree-like neurons

We identified six types of lobula-specific VPNs that have tangential or tree-like arborizations and termed them LT1, 10–12, 31, and 32. Numbers 2–9 were skipped to avoid confusion with the Lt2–9 neurons, for which innervation patterns have partially been described (Fischbach and Dittrich, 1989).

LT1. LT1 consists of four neurons that have their cell bodies in the anterior dorsal area of the lateral cell body region (Figs. 5D–F, 9A–C, 17A). This pathway has been identified as Lt1 (lobula tangential 1) (Fischbach and Dittrich, 1989). The cell body fibers run toward the lobula neck and bifurcate to project to the lobula and the vlpr (Fig. 9A–C). In the lobula, the fibers initially run along its medial and posterior surface (Figs. 5D, 9C). Upon reaching the posteriormost edge of the lobula, the fibers enter the lobula neuropil to form thin, tangential arborization in the Lo3 layer (Fig. 9B). A single neuron covers the whole visual field (Fig. 5F). In the vlpr, the fiber bundle first projects into the vlpr, makes a steep turn laterally (arrows in Fig. 9A–C), and arborizes in the lateralmost vlpr to form many varicosities. The n-syb::GFP signal was observed only in the vlpr (Fig. 14I), suggesting that LT1 neurons are centripetal (Fig. 6B).

LT10. The LT10 pathway consists of a single neuron (Fig. 9D–F), which is likely identical with Lt10 (Fischbach and Dittrich, 1989). Its cell body is located in the anterior dorsal area of the lateral cell body region (Fig. 17A). The cell body fiber runs toward the lobula neck, from where the fiber runs dorsally to project to the dorsal part of the lobula. The fiber forms branches at the dorsalmost edge of the lobula and sends tangential arborizations dorsoventrally along the Lo4 layer (Fig. 9E). The arborization covers only the dorsal half of the visual field (Fig. 9D). Horizontally it covers the whole visual field (Figs. 9F, 13A).

The fiber toward the vlpr runs along the lateral edge of the vlpr (Figs. 9F, 13A) and terminates in the dorsolateral vlpr, roughly at the same area as the target of the LT1 and LT11 (Fig. 17B,C). Presynaptic sites were observed only in the vlpr (Fig. 14J), suggesting that it is a centripetal neuron (Fig. 6B).

LT11. The LT11 pathway also consists of a single neuron. The cell body is located in the anterior dorsal area of the lateral cell body region (Figs. 9G–I, 17A). The neuron has tree-like branches in the lobula and form varicosities

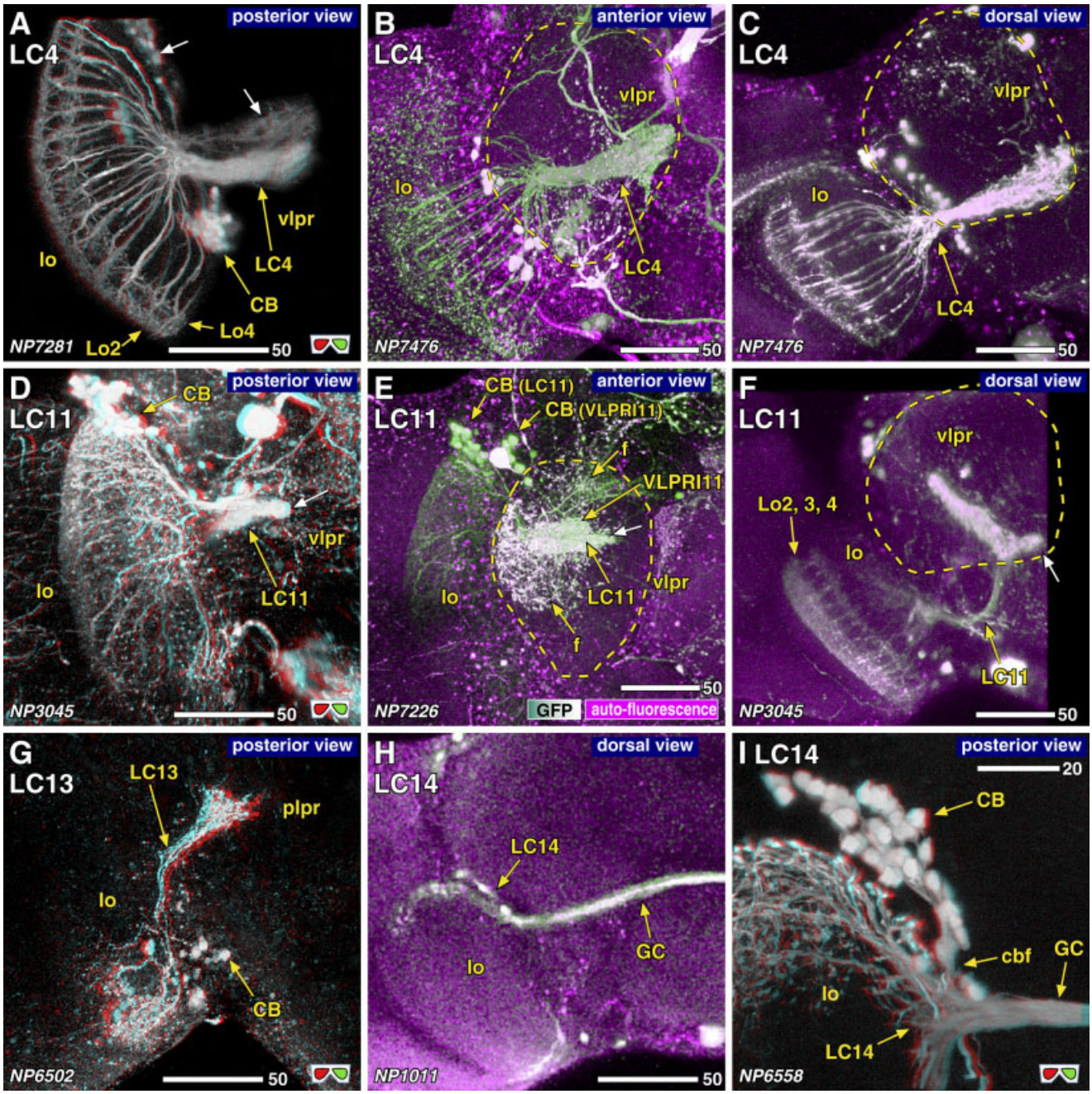

Fig. 11. Detailed arborization patterns of LC4, 11, 13, and 14. **A–C:** LC4. **D–F:** LC11. Dashed lines indicate the contour of the vlpr. White arrows in A indicate the cell bodies and the projection targets of the columnar VPNs arborizing lobula and lobula plate (CC VPNs). White arrow in D–F indicates the edge of the stick-like arborization of LC11. "f" in E indicates the fan-like projections with scattered varicosities that belong to the vlpr intrinsic neuron (VLPRI11). **G:** LC13, showing the arborization confined in the ventralmost area of the lobula. **H,I:** Sections of LC14 at the level of the GC, showing the arborization confined in the peripheral part of the lobula. Erased cells: A: CT, PC, and MT; G: MT and medulla interneurons projecting to lobula. Signals remained in the lobula: A: CC; B, C: medulla intrinsic neurons; E: VLPRI11. Scale bars = 50 μm in A–H; 20 μm in I.

in two separate layers (Figs. 5G,H, 13B). The outer (lateral) layer corresponds to the Lo3 and 4, and the inner (medial) layer corresponds to Lo5 (Fig. 9H). In the vlpr the neuron arborizes in roughly the same anterior dorsal area as that of the LT1 (Fig. 17B,C).

The presynaptic sites are found in the Lo3 and 4 layers of the lobula as well as in the vlpr (Fig. 4E). The varicosities in the Lo5 layer are devoid of n-syb::GFP and are hence likely to be postsynaptic. The LT11 neuron therefore seems to collect information in the Lo5 layer and transmit the signal centrifugally to the Lo3, 4 layers and centripetally to the vlpr (Fig. 6B).

LT12. The LT12 also consists of a single neuron, with its cell body in the anterior area of the lateral cell body

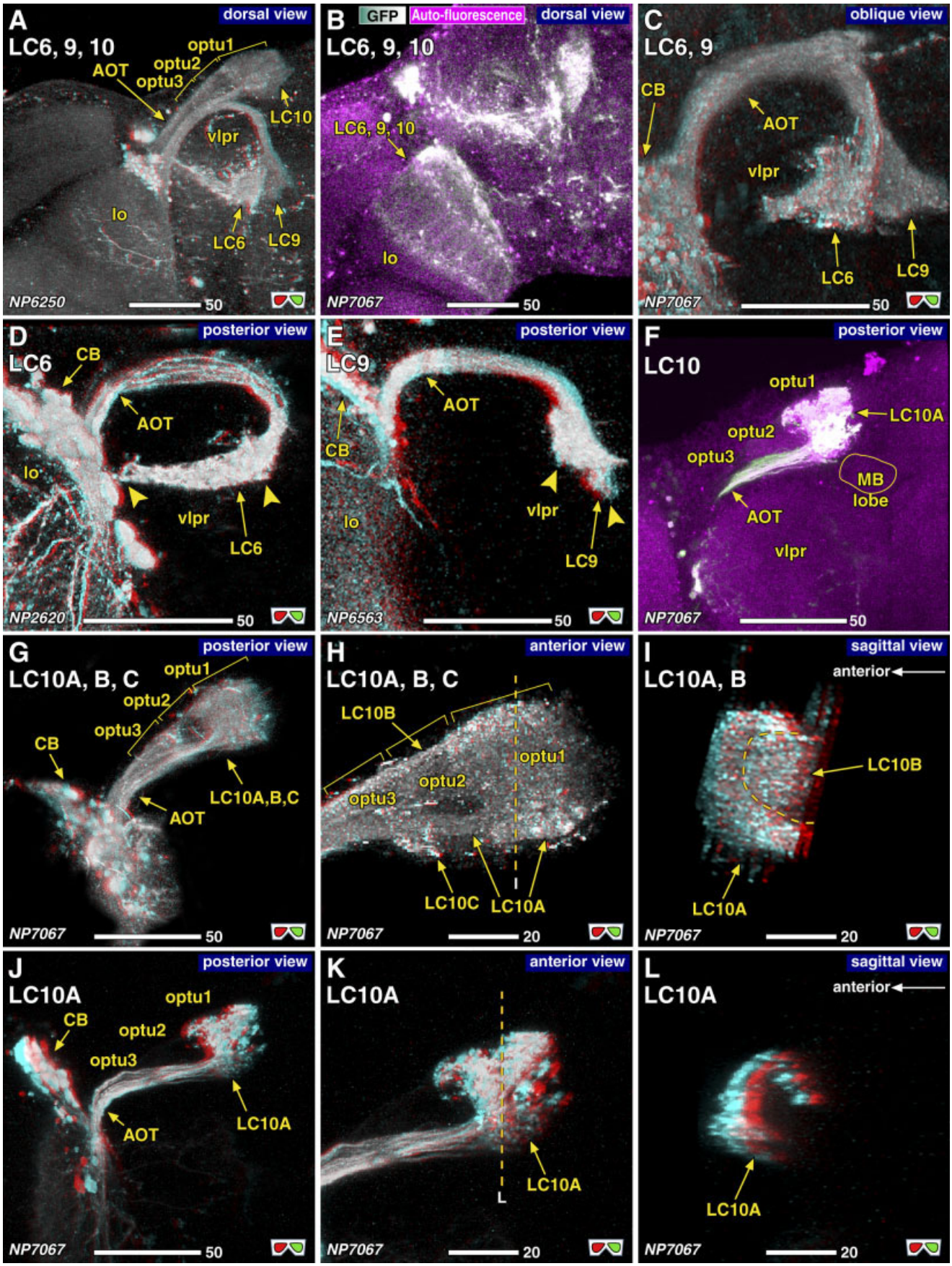

Fig. 12. Detailed arborization patterns of LC6, 9, and 10. **A–C:** Combined staining of LC6, 9, and 10, showing the spatial relationship of each pathway. **D:** LC6 and **E:** LC9 showing the terminal arborization in the vlpr. Arrowheads indicate the edges of the terminal arborization. **F–L:** Innervation of LC10 in the optu. Dashed lines in H and K indicate the position of the cross section shown in I and L, respectively. Dashed lines in I indicates the border between the arborizations of LC10A and LC10B. UAS-*DsRed* was used in D–G and J–L. Erased cells: C: LC10; D: LC4, LC14, MT, and PC; E: faint signal of LC10, PT, and unidentifiable LT; H,I: LC6 and 9. Signals remained in the lobula: A: LT1 and unidentifiable LT. Scale bars = 50 μm in A–G,J; 20 μm in H,I,K,L.

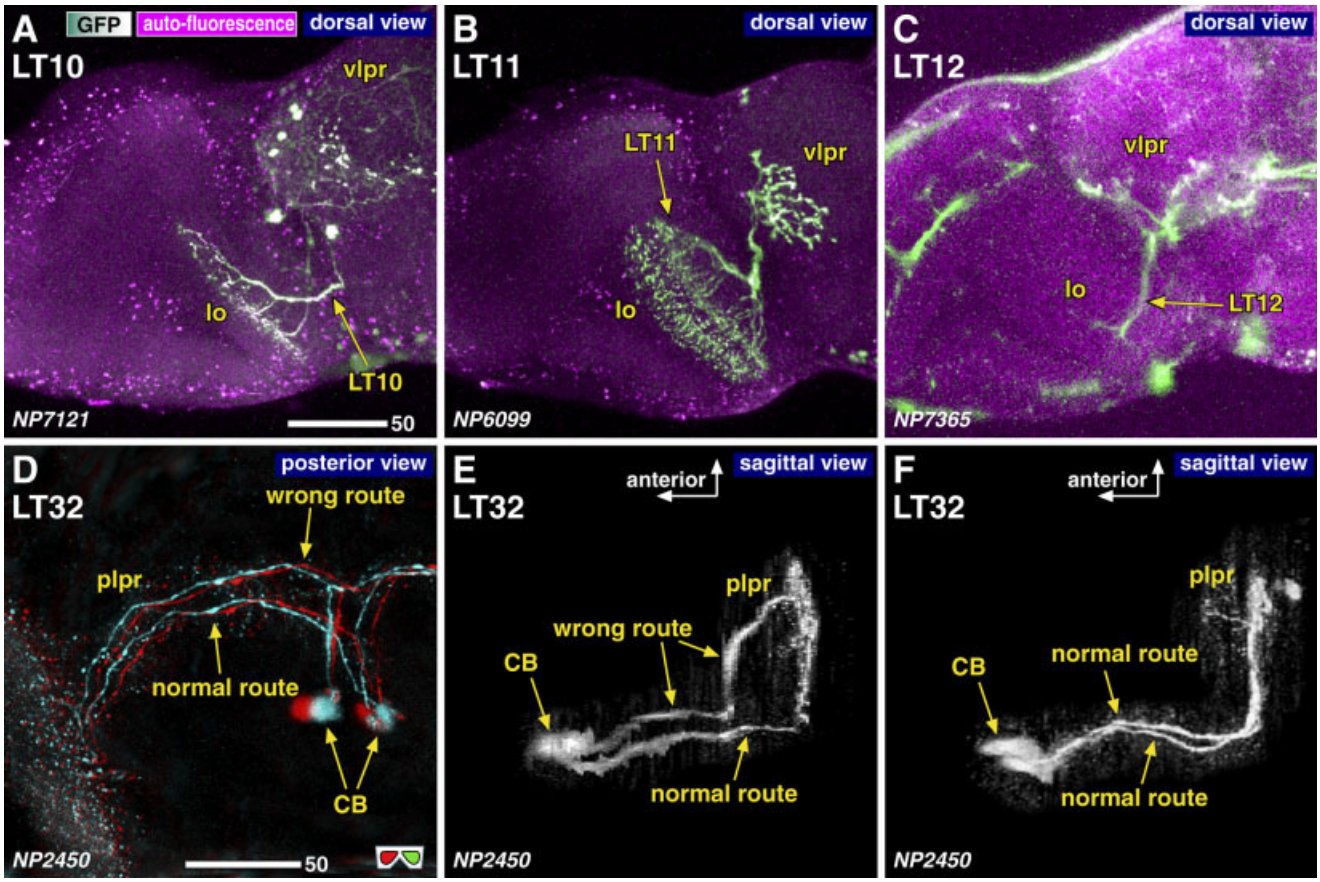

Fig. 13. Detailed arborization patterns of LT10–12 and LT32. **A–C:** Dorsal view of LT10–12, showing tangential (A,C) and tree-like (B) arborization. Note the arborization of LT12 confined in the posterior half of the lobula (C). **D,E:** A sample in which LT32 of one hemisphere took a wrong route to innervate. **F:** Normal route of LT32. UAS-*DsRed* was used in D and E. Erased cells: E, F: MT. Scale bars = 50 μm.

region (Figs. 9J–L, 17A). The cell body fiber bifurcates at the neck of the lobula. The branch toward the lobula arborizes at the posterior edge of the lobula and enters the neuropil tangentially in the Lo4 layer (Fig. 9K). The area of arborization is limited only in the posterior half of the visual field (Fig. 9L). The branch toward the central brain projects to the vlpr along the lobula/lobula plate bundle (Fig. 9J–L). It terminates in the medial vlpr without forming intense branches (Fig. 14K).

The n-syb::GFP signal was observed only in the vlpr (Fig. 14K). Like LT1, 10, and 11, LT12 is therefore centripetal (Fig. 6B).

LT31. We identified only two types of lobula-specific VPNs whose cell bodies lie in the central brain. The first type, LT31, consists of a single neuron. The cell body lies in the central brain cortex posterior to the plpr (Fig. 10A–C). The cell body fiber runs anteriorly straight through the plpr neuropil, and bifurcates in the vlpr (arrowhead in Fig. 10A–C). The lateral branch makes a round turn and runs ventral-posteriorly toward the neck of the lobula. From there the neuron forms extensive tree-like branches with varicosities confined in the Lo4 layer. The medial branch makes a right-angle turn (arrow in Fig. 10A–C) to run ventral-posteriorly towards the posterior plpr. It forms terminal arborizations in the area that is close to the position of the cell body (Fig. 10C). Although the distance between the two areas of arborization (plpr and lo) is fairly close, the neuron makes a long U-shaped detour to connect them.

The n-syb::GFP signal of LT31 was observed only in the lobula (Fig. 14F). Arborization in the plpr is devoid of presynapses. There were no varicosities along the trajectory through the vlpr. The LT31 neuron is therefore centrifugal, sending information from the plpr to the Lo4 layer of the lobula (Fig. 6B).

LT32. The LT32 pathway also consists of a single neuron per hemisphere (Fig. 10D–F). A pair of cell bodies lies on each side of the esophageal foramen. The cell body fiber runs posteriorly along the oesophagus, and turns upwards near the posterior end of the brain (Fig. 13F). There the fiber forms a Y-shaped branch (arrowheads in Figs. 10D, 14L). One branch runs laterally to project to the lobula, and the other crosses the midline to innervate the contralateral lobula. Along the trajectory towards the lobula, the fiber forms another collateral branch (white arrows in Fig. 10D–F), which innervates the plpr and forms fine arborizations. The main branch reaches the lobula and forms extensive tree-like arborizations with varicosities in the Lo5 and 6 layers (Fig. 10E).

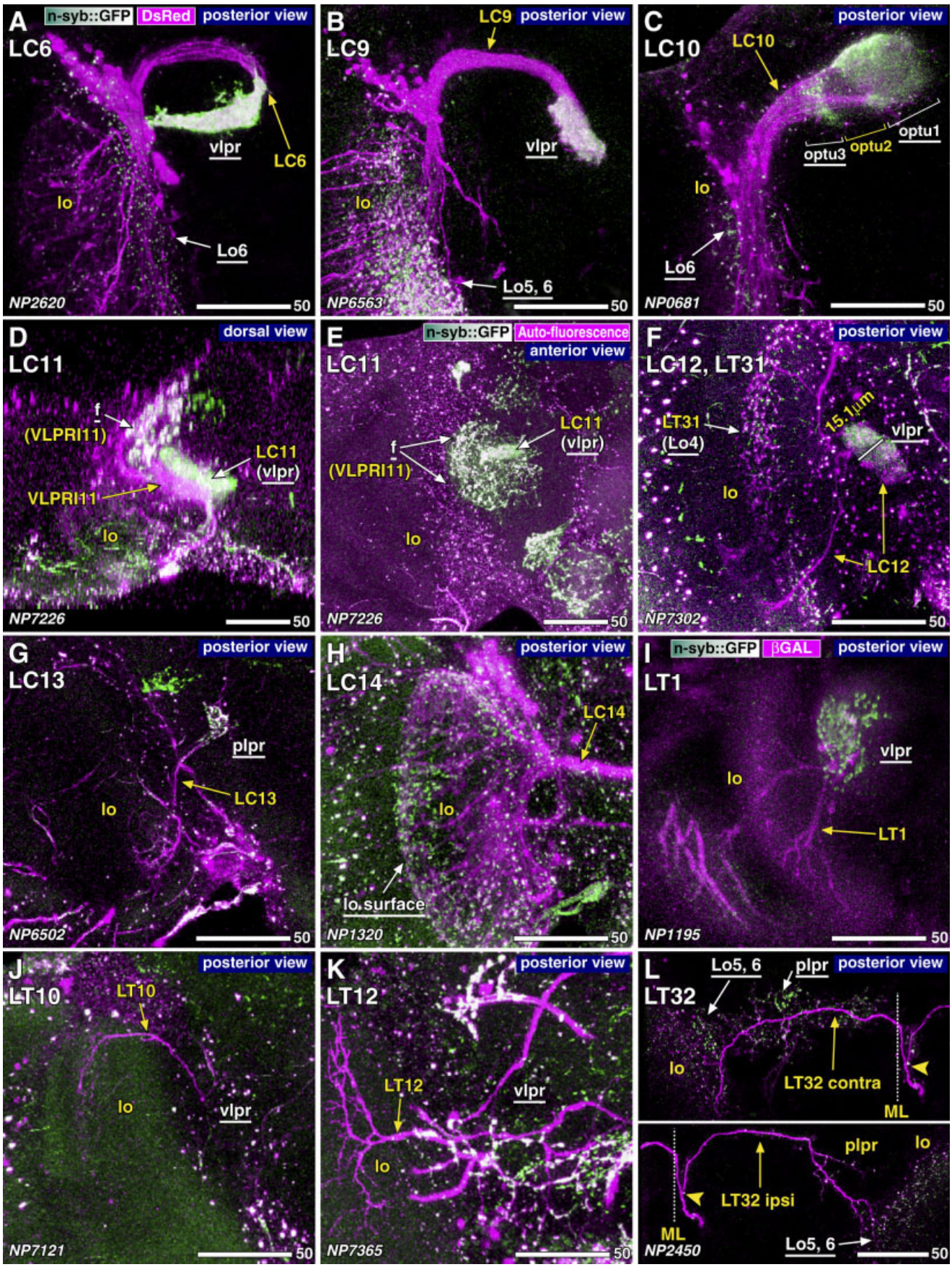
A
n-syb::GFP
DsRed
posterior view
LC6
vlpr
LC6
lo
Lo6
NP2620
50
B
LC9
posterior view
LC9
vlpr
lo
Lo5, 6
NP6563
50
C
posterior view
LC10
LC10
optu1
optu3
optu2
lo
Lo6
NP0681
50
D
dorsal view
LC11
f
(VLPRI11)
LC11
(vlpr)
VLPRI11
lo
NP7226
50
E
n-syb::GFP
Auto-fluorescence
anterior view
LC11
LC11
(vlpr)
f
(VLPRI11)
lo
NP7226
50
F
posterior view
LC12, LT31
LT31
(Lo4)
15.1µm
vlpr
lo
LC12
NP7302
50
G
posterior view
LC13
plpr
LC13
lo
NP6502
50
H
posterior view
LC14
LC14
lo
lo surface
NP1320
50
I
n-syb::GFP
βGAL
posterior view
LT1
vlpr
lo
LT1
NP1195
50
J
posterior view
LT10
LT10
lo
vlpr
NP7121
50
K
posterior view
LT12
LT12
vlpr
lo
NP7365
50
L
Lo5, 6
plpr
posterior view
LT32
lo
LT32 contra
ML
plpr
lo
LT32 ipsi
ML
NP2450
Lo5, 6
50

Figure 14

We also found an interesting example of misrouting projections. In one sample the cell body fiber of one side of the LT32 turns upward prematurely before the fiber reaches the posterior end of the brain (Fig. 13D,E). The misrouted projection nevertheless turns again posteriorly to reach the posterior surface of the brain. The fiber forms the Y-shaped branch and innervates the plpr and lobula-like normal neurons. This suggests that the fibers of LT32 have the ability to find the correct projection target even when the fiber lost its way in the complex neuropil structure.

Because LT32 neurons on both hemispheres project along almost the same trajectory, it is difficult to identify the presynaptic sites of the neuron of a particular hemisphere. Fortunately, we found one sample in which DsRed failed to express in one of the LT32 neurons (Fig. 14L). In the contralateral side of the projection (Fig. 14L, top), extensive distribution of presynapses was observed in the plpr as well as in the lobula. In the ipsilateral side (Fig. 14L, bottom), the plpr is essentially devoid of presynapses, although there are arborizations. Presynapses are observed only in the lobula. Thus, it is likely that LT32 collect information in the ipsilateral plpr and send the signal to the lobulae on both hemispheres as well as to the contralateral plpr (Fig. 6B).

DISCUSSION

In this study we performed a systematic identification of the projection neurons connecting the optic lobe and the central brain. Among the 44 types of VPNs we identified, 24 are associated with the lobula (lobula VPNs). Fourteen of them arborize specifically in the lobula (lobula-specific VPNs), whereas the other 10 contribute not only to the lobula but also to the medulla and/or lobula plate (complex VPNs). Because the latter type of the lobula VPNs will be described in the next article (Part II), functional implications and systematic comparison of the identified neural circuits connecting the lobula and the central brain will be discussed collectively there. Here we limit our discussion to the technical aspects of the experimental approach, as well as to the issues that specifically concern the lobula-specific VPNs.

Advantage of the molecular genetic cell-labeling technique

Although previous studies provide comprehensive descriptions of the local neurons and interneurons of the *Drosophila* optic lobe (Power, 1943; Fischbach and Dittrich, 1989; Bausenwein et al., 1992), structural information about the VPNs has been relatively limited. Compared to the local and interneurons in the optic lobe, VPNs generally have long axons. The Golgi impregnation technique has an inherent drawback to label such cells. A prolonged incubation time is required for completing silver-mirror reaction throughout long neural fibers. This, however, results in the staining of a larger number of neurons, making it difficult to discriminate each labeled cell. If the incubation time is kept short to increase the specificity of the staining, some parts of the neural fibers tend to be left unlabeled. For example, it is often difficult to trace axons to identify the projection targets and cell body fibers to reveal the location of the cell bodies, if they are detached from the area of the primary arborization.

Although the dye infiltration technique does not suffer from this problem, application of dye is limited to the cells that are easy to access. Neurons that run deep within the neuropils, such as the VPNs emerging from lobula, are difficult to label with this technique. Antibody staining can label only limited types of VPNs for which convenient antibodies are available. Generation of a large variety of good antibodies turned out to be very difficult. Also, the arborization pattern of the labeled cells cannot be visualized if the obtained antibody recognizes molecules that exist only in the cell body or in particular subregions of the neural fibers.

The molecular genetic cell labeling technique featuring GAL4 enhancer-trap strains (Brand and Perrimon, 1993) has various advantages over these traditional techniques. Generating a large variety of enhancer-trap lines is much easier than generating the same variety of antibodies. The morphology of the GAL4-expressing cells can be visualized with a wide variety of reporter strains that label either all or specific substructures of the labeled cells (Ito et al., 2003). Whereas Golgi impregnation and dye infiltration techniques label neurons stochastically, enhancer-trap lines can label identical sets of cells reproducibly among individuals. In addition, each enhancer-trap strain labels all the cells that share the same pattern of enhancer activity, giving a clue about the total number of the cells that belong to a particular cell category.

Using a smaller number of GAL4 strains, a comprehensive identification of larval glial cells (Ito et al., 1995) and extensive if not comprehensive identification of the intrinsic and extrinsic neurons of the mushroom bodies (Ito et al., 1997, 1998) have been performed previously. Because the adult brain has a very complicated structure, however, systematic identification of the neural circuits has not been practical. The generation of the large collection of NP GAL4 strains (Yoshihara and Ito, 2000; Hayashi et al., 2002) has made such an endeavor a feasible project.

Direction of information estimated by the distribution of the presynaptic sites

One of the advantages of using GAL4 enhancer-trap strains is that it is easy to drive expression of more than one reporter gene in the labeled cells. We took advantage of this to label the overall morphology of the cells and the distribution of the presynaptic sites simultaneously. Although n-syb::GFP is a potent marker of presynapses (Ito et al., 1998), it visualizes only the tips of the neural fibers, making it difficult to understand the distribution of the presynapses in the context of the overall fiber structure.

Fig. 14. Distribution of the presynaptic sites. Staining with the presynaptic site-targeted n-syb::GFP (green to white) and cytoplasmic DsRed (magenta). White characters with an underline indicate the areas of arborizations with presynaptic sites. In **B,** the n-syb signal observed in Lo5 and 6 layers could not be confirmed as deriving from the LC9 neurons, because the Y cells, which project from the medulla to the lobula and lobula plate, also terminate in these layers. In **D,E,** arborizations of the vlpr intrinsic neurons VLPRI11 are also shown ("f"). In **I,** UAS-*lacZ* was used for visualizing the cells because the flies become lethal when this GAL4 line is crossed with UAS-*DsRed*. ML; midline. Erased cells: **A:** LC4, LC14, MT, and PC; B: faint LC10, PT, and unidentifiable LT; I: MT, HS, and VS; **J:** MT and unidentifiable LT; **K:** PT and MT; **L:** MT. Signals remained in the lobula: A: LC4 and LC14; B: Y cell, faint LC10 and unidentifiable LT. **H:** MT and a variant of LC14 to medulla; I: VS; K: Axons of PT in the central brain. Scale bars = 50 μm.

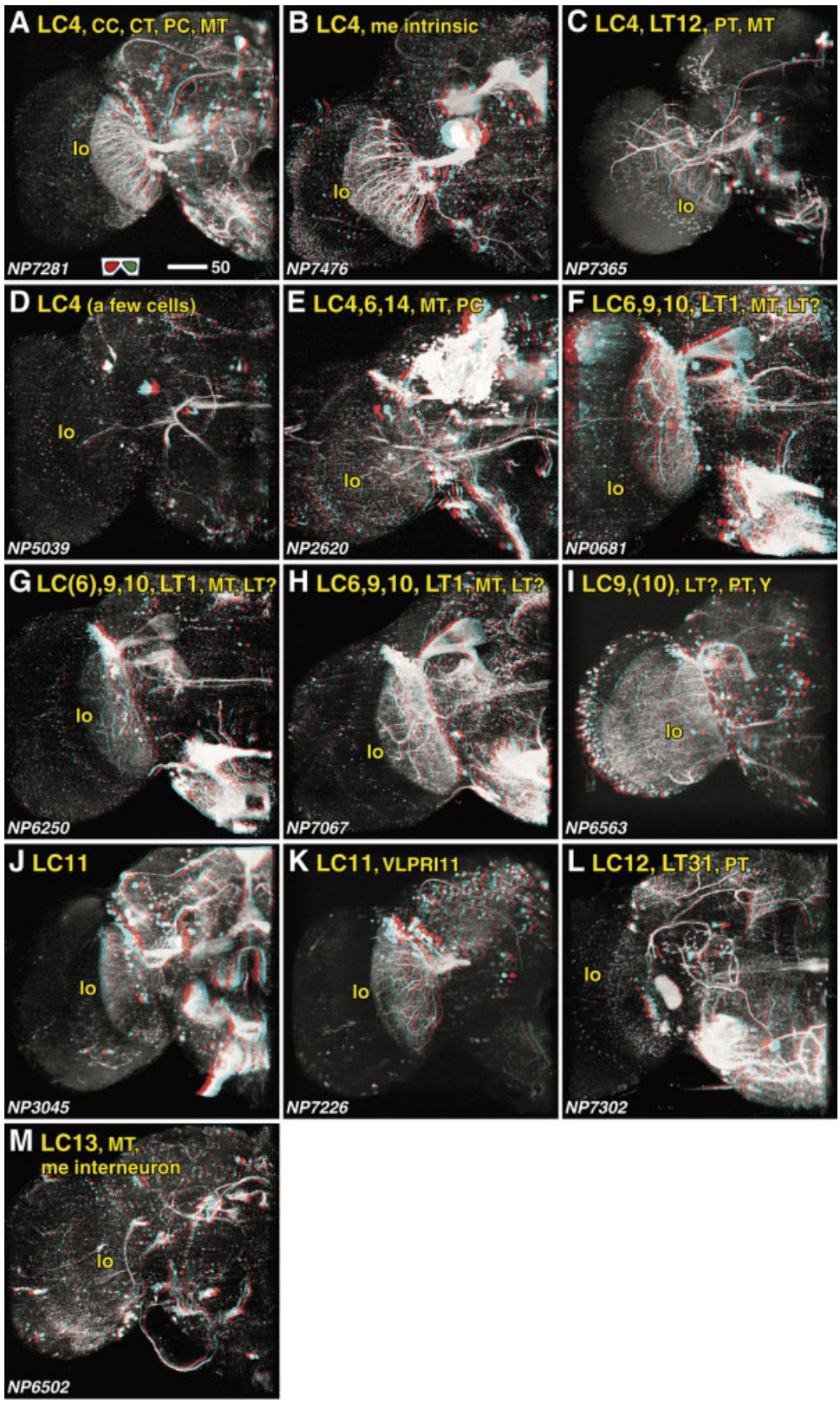

Figs. 15, 16. Expression pattern of the GAL4 enhancer-trap strains used in this study. All the strains express GAL4 in various other neurons than the lobula-specific VPNs. Types of the cells labeled in the optic lobe are shown in each panel (see Table 2 for details). Question marks indicate unidentifiable LT neurons. Labeled cells in the central brain are not described. When using these strains for behavioral analyses with ectopic expression of effector genes, special care should be taken to assess the effect of gene expression in these non-VPN cells. Scale bars = 50 μm.

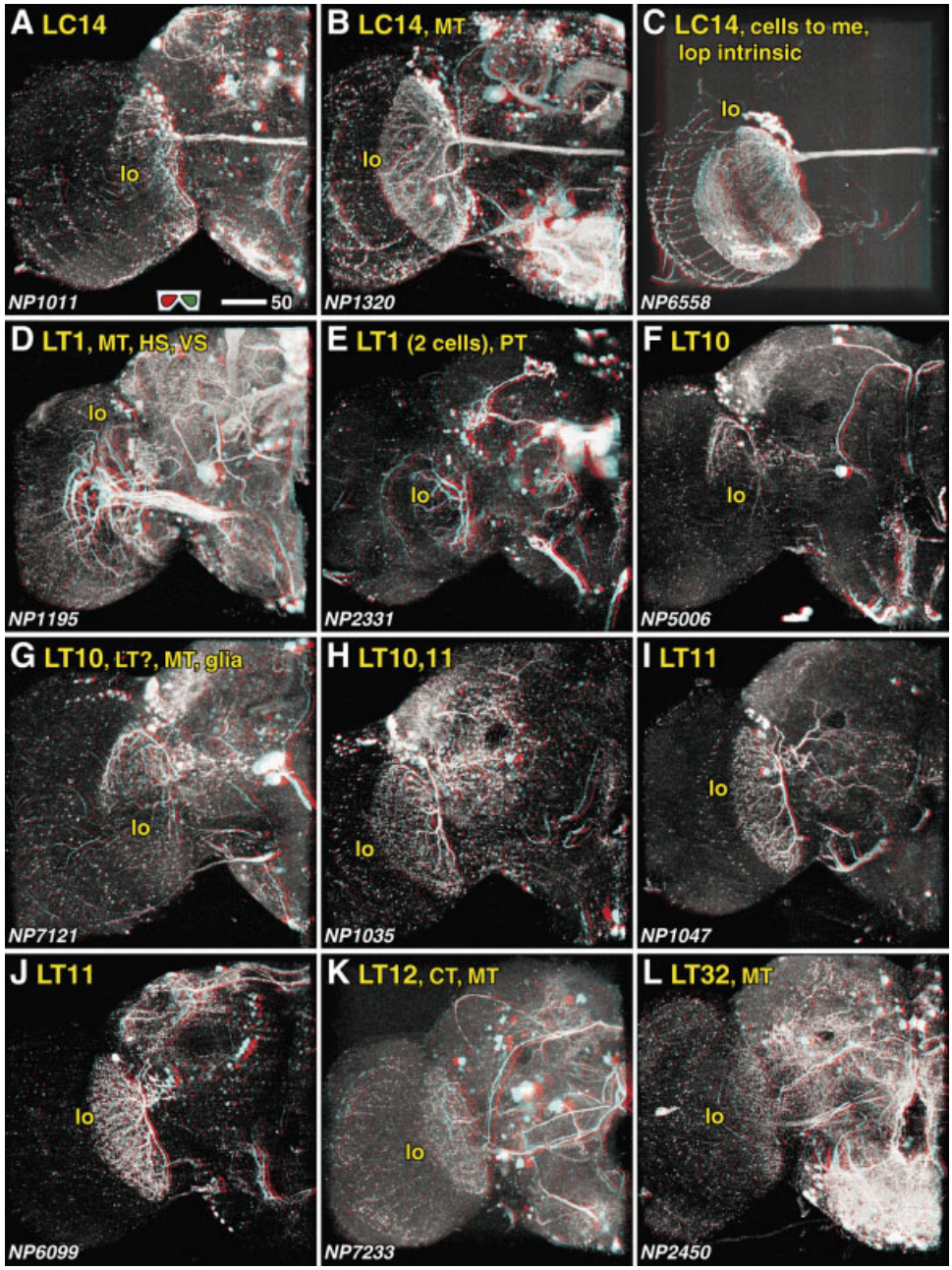

Figure 16

To obtain a novel fluorescent reporter that can be used simultaneously with n-syb::GFP, we developed a reporter featuring coral-derived red fluorescent protein DsRed (Verkhusha et al., 2001). Unlike GFP, DsRed forms a tetramer in the cells. This is not suitable for making fusion constructs featuring DsRed, because such proteins tend to aggregate in the cells and disrupt the intracellular structure. On the other hand, DsRed itself diffuses evenly in the cytoplasm of both cell bodies and long neural fibers, making it an ideal reporter for visualizing the overall projection pattern of the labeled cells.

Double labeling with DsRed and n-syb::GFP revealed that certain parts of the neural fibers are not labeled with n-syb::GFP, even though extensive arborizations and varicosity-like structures are visualized with DsRed. Because n-syb should exist in all the presynaptic sites where docking of the synaptic vesicles occur, it is likely that postsynaptic sites are distributed in these fiber branches. Although it is possible that arborizations that are rich in presynaptic sites may also have postsynaptic sites in the same fiber branches, it should be reasonable to assume as a first approximation that the regions of extensive arborizations that are devoid of presynapses would be the primary input sites of the labeled neurons. This way, we were able to estimate the direction of information in each identified VPN.

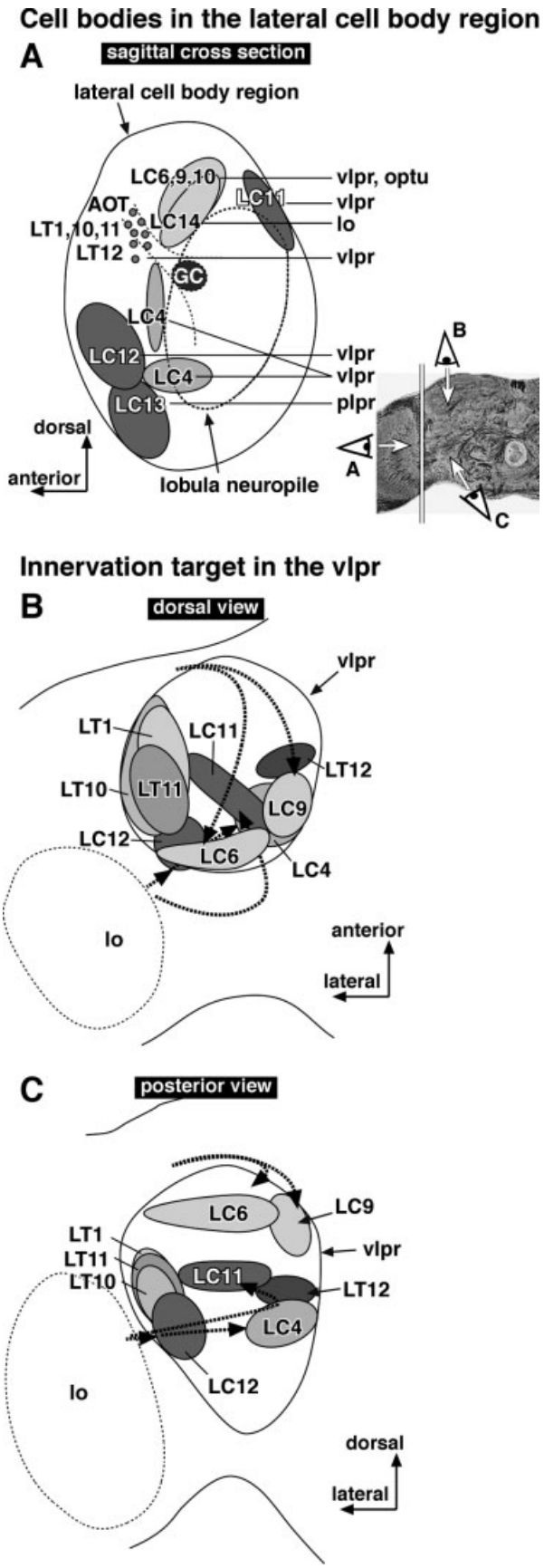

Systematic identification of the VPNs

In this study we identified 14 pathways of the lobula-specific VPNs (Table1). The set of VPNs we identified include many of the lobula-specific VPNs that have been described previously in the *Drosophila* brain using various staining methods (Power, 1943; Fischbach, 1983; Fischbach and Lyly-Hünerberg, 1983; Fischbach and Dittrich, 1989; Morales et al., 2002). In particular, Fischbach and Dittrich (1989) reported 17 types of lobula-specific VPNs. Based on the arborization pattern in the lobula and the projection in the central brain, we concluded that LC4, 6, and LT1, 10 were identical with Lcn4, 6, and Lt1, 10 described in their study. Unambiguous comparison was difficult for the remaining 13 types of VPNs because the previous study described only projections within the lobula. It is possible that LC11, 12, and 13 might correspond to Lcn7, 8, and 2, respectively, because these pairs of VPNs arborize in similar layers of the lobula. Similarly, Lt4, 5, and 7 might correspond to LT32, CT31, and CT2 (the latter two will be described in our next article). In these cases we assigned numbers that do not overlap with the previous study because the identity could not be confirmed without a comparison of the projection targets in the central brain.

There are still several types of VPNs that were described in Fischbach and Dittrich (1989) but not identified in our study (Lcn1, 5, and Lt2, 3, 6, 8, 9). In addition to the 44 VPN pathways we identified, there were several types of candidate VPNs that we noticed but could not identify with confidence because labeling of other neurons obscures their arborization and trajectory in the optic lobe and in the central brain neuropils. Most of these candidate VPNs consist of thin bundles of fibers originating from a small number of cell bodies. They are therefore likely to be the tangential or tree-like type, with only a few cell bodies per pathway. Some of these pathways might correspond to the unaccounted Lt neurons listed above.

The repertoire of the GAL4 enhancer-trap strains we used for the screening collectively covers about 2,000 genetic loci, one-seventh the total number of the gene (Hayashi et al., 2002). The P-element transposon tends to jump preferentially into specific genetic loci, the so-called hot spots. Interestingly, different strains that have their GAL4 insertions in the same genetic locus but at slightly different positions may sometimes show slightly different expression patterns. For example, although the GAL4 insertion points of NP0681, NP6250, and NP7067 strains are very close to each other, NP6250 labels LC6 neurons only faintly, whereas the others label them strongly (Table 2; Fig. 15).

Nevertheless, the variety of the observed GAL4 expression patterns may not cover all the patterns that are possible to occur in the *Drosophila* genome. However, for

Fig. 17. Summary of the distribution of the cell bodies and the innervation targets in the vlpr. The small photograph indicates the direction of the view of each panel. The white line indicates the position of the sagittal section show in **A.** A: Location of the cell bodies in the lateral cell body region (LCBR in Fig. 1A). Circles represent the clusters of VPN cell bodies. Abbreviations on the right indicate the projection target of each VPN pathway. **B,C:** Innervation target regions in the vlpr. Circles represent the area in which VPNs terminate. Dotted arrows indicate the trajectory of the VPN pathways.

most of the 14 identified VPN types, we found more than one strain that labels respective VPNs. It is therefore likely that the screening we performed is near saturation. Even if we generate and screen much more GAL4 strains, it is not likely that we would find a considerable number of novel pathways.

Because the GAL4 enhancer-trap system relies on the activity of the enhancers to label cells, neurons that tend to share the same enhancer activity cannot be labeled specifically. This causes two practical problems. First, it is sometimes very difficult to label a desired subpopulation of VPNs selectively. For example, in spite of our extensive screening we could not identify the GAL4 strains that specifically label LC6, 9, and 10 pathways or each subtype of LC10A, B, and C neurons separately. Second, certain populations of VPNs may not be labeled specifically, and might therefore have escaped our identification if they share enhancer activity patterns with many other neurons in and near the lobula neuropil. In such cases, massive labeling of adjacent cell populations would obscure the trajectories of the candidate VPNs.

An important type of VPN that was not identified in our screening is the 5-HT immunoreactive neurons, which have extensive tree-like arborizations in the lobula as well as in other optic lobe neuropils (Nässel, 1988; Meinertzhagen and Hanson, 1993). It is likely that none of our GAL4 strains hit the genetic loci that are associated with 5-HT.

Male-specific lobula giant neurons (MLG) have been observed in the lobula of larger flies such as *Sarcophaga bullata* and *Calliphora erythrocephala* (Gilbert and Strausfeld, 1991; Gronenberg and Strausfeld, 1991; Strausfeld, 1991). Because we observed the brains of only female flies in the current study, it is possible that we might have overlooked such neurons. Considering that the GAL4 strains label neurons genetically, it is feasible to compare the projection pattern and the number of labeled cells between sexes. Indeed, our screening yielded a GAL4 line that labels sexually dimorphic neurons, albeit not in the visual system (Kimura et al., 2005). It is not very likely, however, that the *Drosophila* lobula would have extensive male-specific neural circuits. In the fly species in which male flies chase flying females during courtship, male compound eyes are larger and cover the anterior area of the head capsule for stereographic eyesight. In *Drosophila*, in which male flies court walking females, male compound eyes are smaller than in females and are separated on both sides of the head, just like the female eyes. Thus, the male-specific stereographic visual field, with which male lobula giant neurons of larger flies are associated, may not exist in the *Drosophila* visual system.

Various types of columnar lobula neurons (col) have also been identified in these larger flies. The bistratified arborization in the lobula and relatively straight trajectory in the vlpr suggest that the LC4 we identified might correspond to the col A neurons (Hausen and Egelhaaf, 1989; Gilbert and Strausfeld, 1991), although we have not examined the direct connectivity between LC4 and giant descending neurons, a characteristic of col A. Because none of the identified lobula-specific columnar VPNs cross the midline, we did not find neurons that would correspond to col B neurons (Gilbert and Strausfeld, 1991). Strausfeld (1976) documented seven types of columnar VPNs (neurons 1–7) in the brain of *Musca domestica*. Among them, neuron #3 may correspond to the LC4, and #4 appears similar to LC13. Other LC neurons we identified do not exactly match the neurons described in this study.

Variability of the labeled cell numbers

For each type of VPN we compared the number of labeled cells in three individuals (Table 2). In the VPN types that consist of less than five cells, the number of labeled cells was the same for all the samples examined, suggesting that the number of cells per VPN type is strictly regulated. For the VPNs whose cell number exceeds 10 neurons, on the other hand, there were fluctuations among individuals. The difference was small, however: the ratio between the mean and the standard deviation was less than 10% in all cases.

There are two possibilities to explain this variability. First, the number of the VPNs itself might be variable among individuals. Or, second, the cell number is consistent but the inserted GAL4 gene might have failed to drive the UAS-linked reporter in some cells. Although the former seems to be more likely, the latter also happens occasionally. When metameric glial cells in the larval ventral nerve cord were visualized using GAL4 enhancer-trap strains (Ito et al., 1995), glial cells in a few segments of some preparations were left unlabeled stochastically, although Nomarski optics visualized the existence of the glial cells in that location.

It is important to note that the entire population of neurons of a particular structural category may not be labeled simultaneously with a single GAL4 strain. For example, the GAL4 strains that label the largest subset of the olfactory projection neurons from the antennal lobe to the lateral horn (GH146 and NP225) label only 70–90 neurons, although there are an estimated 150–200 cells in this pathway (Stocker et al., 1997; Wong et al., 2002; Tanaka et al., 2004). This may also be the case in the visual neurons. Electron microscopic study revealed that there are ~1,200 fibers in the AOT (Fischbach and Lyly-Hünerberg, 1983). Among them, 100–110 neurons (S1 neurons) are not associated with the optic lobe. The S2 (7–8 cells), S3 (~430 cells), and S4 (~660 cells) are likely associated with the optic lobe. Compared to this, we found only ~330 neurons arising from the lobula (LC6, 9, 10) and a couple of hundred of neurons arising from both the medulla and lobula, which will be described in Part II of our study. Thus, the total number of identified VPNs is still fewer than the number of the fibers observed in the AOT cross-section. There are two possibilities to explain this discrepancy. First, the unaccounted-for neurons may actually derive from the central brain like the S1 neurons. Or, second, certain types of VPNs in the AOT are not labeled with the current set of GAL4 strains. Therefore, the cell counts described here might better be regarded as the minimum number of cells that belong to the particular VPN pathway.

Mapping system of the central brain neuropils

In this study we introduced a canonical naming scheme for describing the location of the central brain neuropils unambiguously. Using two landmarks that are easily identifiable even without staining, the mushroom body and the great commissure, we divided the protocerebrum other than the AL, MB, and CC into 16 blocks (Figs. 2, 3). The purpose of this canonical terminology is to provide a framework with which innervation targets of different

neurons described in different studies can be compared systematically. For two types of neurons to have a direct synaptic connection, it is a prerequisite that they arborize in the same block of the neuropil.

It is important to note that there is no apparent correlation between these neuropil blocks and the functional units of the neural circuitry modules. Studies on the structure and function of the brain are confronted by a kind of chicken-and-egg situation: A clear nomenclature is required for describing the functional segregation of the brain, whereas detailed knowledge about the functional segregation is required for determining the brain units. Unlike mammalian cerebral cortex, the insect central brain does not consist of simple, layered structures. Neural circuits crisscross so extensively that a discernible structural border hardly exists. This makes it impossible to subdivide the insect brain into "areas" like Brodmann (1909) did for the mammalian brains. We reasoned that a feasible compromise in such a situation would be to rely on an arbitrary mapping system that we propose in this study until sufficient anatomical and functional data accumulate.

Arborization of the lobula-specific VPNs in the optic lobe

The projection patterns of the 14 lobula-specific VPNs can be classified in several ways (Table 1; Fig. 6B). First, there are eight types of columnar VPNs and six types of tangential or tree-like VPNs. Whereas the total number of the columnar VPNs is ~490, there are only nine tangential/tree-like VPNs. Thus, most of the lobula-specific VPNs are columnar. On the other hand, among the 10 complex-type VPNs associated with the lobula, which contribute not only to the lobula but also to the medulla and/or lobula plate, seven are tangential/tree-like and only three are columnar (see Part II, upcoming).

A single tangential/tree-like pathway consists of only a few neurons (either one or four). A columnar pathway, on the other hand, consists of tens of neurons. Although the LC13 pathway consists of only 16 cells, the LC6, 9, and 10 pathways are likely to be comprised of as many as 80–150 neurons. These numbers, however, are much fewer than the number of ommatidia (~780 in female). Although the total cell count of some pathways might be larger than that of the labeled cells (discussed above), it is not likely that any VPN pathway consists of as many cells as the number of ommatidia. Therefore, the spatial resolution of the fly vision would be reduced significantly when the visual information is conveyed from the lobula to the central brain.

VPNs can also be classified by the position of the cell bodies. Twelve out of the 14 types have their cell bodies in the lateral cell body region (Fig. 17A). The cell bodies of the columnar VPNs are clustered in the dorsal and ventral areas, whereas those of the tangential and tree-like VPNs are accumulated in the anterior-dorsal region. They all extend their cell body fibers toward the neck of the lobula, where the fibers bifurcate to project to the lobula and the central brain. Although these cell bodies lie directly adjacent to the lobula neuropil, there is no neuron that projects directly from the lateral cell body region to lobula without going via the lobula neck.

Projection targets of the lobula-specific VPNs

The identified lobula-specific VPNs are associated with only three central brain regions: plpr, optu, and vlpr. The plpr receives centripetal information via a columnar pathway LC13 and send centrifugal signal via tree-like LT31 and LT32. The arborization areas of LC13, LT31, and LT32, however, do not seem to overlap significantly (compare Figs. 8G–I and 10A–F). Although a more detailed analysis would be required to determine the spatial relationship of these neurons, it is probable that LC13 may not form synapses directly onto LT31 and LT32. Therefore, the centrifugal information that lobula receives from the plpr would not be a simple direct feedback of the centripetal signal it sends to the plpr.

The optu is contributed by a single lobula-specific VPN pathway, LC10. Our data suggest that LC10 might be subdivided into at least three types of neurons (LC10A, B, and C), although we could not obtain the GAL4 strains that label each subtype specifically. The terminals of these neurons divide the optic tubercle mediolaterally into smaller subunits: optu1, 2, and 3. LC10C seems to terminate only in optu3, whereas LC10A and 10B terminate in different areas of optu1. Optu2 is devoid of LC10 terminals (Fig. 12G,H).

The optu has a smooth cone-like shape. Such morphology might suggest that the VPN axons project mostly in parallel within the optu. On the contrary, the LC10A neurons run along the ventral edge of the optu and make a steep right-angled turn to innervate the anterior optu1 ventrodorsally (Fig. 12J,K). LC10B, on the other hand, innervates the posterior optu1 lateromedially. The orientations of the terminal arborizations in optu1 would therefore be strikingly different between these subtypes of VPNs.

The optu of the locust *Schistocerca gregaria* has been divided into upper and lower subunits, and the upper unit comprises inner and outer lobes (Homberg et al., 2003). The morphology of the terminals raises the possibility that these two lobes might correspond to optu1 and optu3, respectively. Like the LC10A neurons we identified, arborization in the inner lobe makes a right-angled turn (Homberg et al., 2003). The locust lower unit is reported as being contributed by the neurons originating from both lobula and medulla. We identified a similar VPN pathway in *Drosophila*, which will be discussed in Part II of our study.

The main target of the lobula-specific VPNs is the vlpr; nine out of the 14 pathways terminate in this area. All the pathways are centripetal. Unlike the plpr, the vlpr therefore serves primarily as an input site in relation to the lobula.

The projection patterns within the vlpr are significantly different between pathways (Fig. 17B,C). Among the four tangential pathways, LT1, 10, and 11 terminate in an overlapping lateralmost area of the vlpr. LT12, on the other hand, terminates in the medialmost region. The five columnar VPNs all innervate different subregions of the vlpr. Although the terminals of these VPNs form various morphologies such as a triangle, cone, or stick, they share a common feature that the terminals are confined within relatively small and discrete areas of the central brain. For this matter, these subregions are comparable to the glomerular structure in the antennal lobe and have hence

been described as optic foci or optic glomeruli (Strausfeld, 1976; Strausfeld and Gronenberg, 1990).

The five columnar VPN pathways terminate in as many numbers of the optic glomeruli. Interestingly, these VPNs project to the glomeruli from completely different directions. For example, the optic glomeruli contributed by LC11 and LC12 are adjacent to each other, but the directions of the neural fibers crisscross almost at a right angle. The situation is the same between LC4 and LC9.

Flies as well as many other insects are known to recognize shapes presented in front of their eyes (Chen et al., 2003; Stach et al., 2004; Tang et al., 2004). It is therefore likely that insect brains should possess neural circuits that interpret retinotopic information to extract characteristics of the object shape. Does this process occur in the central brain? Or within the optic lobe? Because each columnar pathway consists of tens of neurons or more, and because each single neuron arborizes only in a small area of the visual field in the lobula, the lobula-specific columnar VPNs would in principle be able to convey retinotopic information to the optic glomeruli, albeit at a relatively low spatial resolution. Neural circuits in the optic glomeruli or in even higher visual centers of the central brain may read this information to extract the characteristics of the object shape. Or, these VPNs might convey information of the already extracted morphological features in the optic lobe, in which case the retinotopic projection map may not be maintained. Our study indicates that these VPNs do not form a single projection map from the lobula to the vlpr. Rather, the retinotopic map, if it is conveyed to the central brain, is likely to be represented redundantly in at least five glomeruli of the *Drosophila* vlpr. Further anatomical and physiological analyses of the lobula-specific columnar VPNs would be important to address this issue.

It is also interesting to note that many parts of the vlpr, such as the core region and the anteriormost and ventralmost areas of the vlpr, do not receive visual information. This suggests that the vlpr might be divided into several functional subunits. Do these areas serve as output areas to other central brain neuropils? Or, do they receive sensory information of other modalities? Analyses of other types of brain neurons would be required to answer these questions.

In this study we performed a systematic identification and description of the VPNs associated specifically with the lobula. Lobula is contributed also by 10 other VPNs that connect not only lobula but also other neuropils of the optic lobe to the central brain. Further analysis of the lobula-specific VPNs will be discussed together with these complex-type VPNs in the next part of our study.

ACKNOWLEDGMENTS

We thank Yasuyoshi Nishida and Motoya Katsuki for generous support at Nagoya University and the National Institute for Basic Biology, respectively. We thank Joachim Urban and Gerhard Technau for MZ series enhancer-trap strains, the members of the NP consortium, and Daisuke Yamamoto for the NP series strains. We thank Yuko Shimada and Daiki Umetsu for fruitful discussion. We also thank the members of our lab, Takeshi Awasaki, Kentaro Kato, Azusa Kamikouchi, Nobuaki Tanaka, Ryuichi Okada, and Yusuke Uchiyama, for intriguing discussion and screening of the fly strains; and Mariko Kamiya, Atsuko Hattori, Miyuki Nakagawa, Sayaka Nakane, Noriko Nishimura, and Kimiko Tanaka for technical assistance.

LITERATURE CITED

Bausenwein B, Fischbach KF. 1992. Activity labeling patterns in the medulla of *Drosophila melanogaster* caused by motion stimuli. Cell Tissue Res 270:25–35.

Bausenwein B, Dittrich APM, Fischbach KF. 1992. The optic lobe of *Drosophila melanogaster*. II. Sorting of retinotopic pathways in the medulla. Cell Tissue Res 267:17–28.

Brand AH, Perrimon N. 1993. Targeted gene expression as a means of altering cell fates and generating dominant phenotypes. Development 118:401–415.

Brodmann K. 1909. Vergleichende Lokalisationslehre der Grosshirnrinde in ihren Prinzipien dargestellt auf Grund des Zellenbaues. Leipzig: Johann Ambrosius Barth.

Buchner E, Buchner S, Bülthoff H. 1984. Identification of [3H]deoxyglucose-labelled interneurons in the fly from serial autoradiographs. Brain Res 305:384–388.

Buchner E, Bader R, Buchner S, Cox J, Emson PC, Flory E, Heizmann CW, Hemm S, Hofbauer A, Oertel WH. 1988. Cell-specific immuno-probes for the brain of normal and mutant *Drosophila melanogaster*. I. Wild-type visual system. Cell Tissue Res 253:357–370.

Chen L, Zhang S, Srinivasan MV. 2003. Global perception in small brains: topological pattern recognition in honey bees. Proc Natl Acad Sci U S A 100:6884–6889.

Douglass JK, Strausfeld NJ. 1996. Visual motion-detection circuits in flies: parallel direction- and non-direction-sensitive pathways between the medulla and lobula plate. J Neurosci 16:4551–4562.

Douglass JK, Strausfeld NJ. 1998. Functionally and anatomically segregated visual pathways in the lobula complex of a calliphorid fly. J Comp Neurol 396:84–104.

Douglass JK, Strausfeld NJ. 2003. Anatomical organization of retinotopic motion-sensitive pathways in the optic lobes of flies. Microsc Res Tech 62:132–150.

Egelhaaf M, Warzecha AK. 1999. Encoding of motion in real time by the fly visual system. Curr Opin Neurobiol 9:454–460.

Estes PS, Ho GLY, Narayanan R, Ramaswami M. 2000. Synaptic localization and restricted diffusion of a *Drosophila* neuronal synaptobrevin-green fluorescent protein chimera in vivo. J Neurogenet 13:233–255.

Feiler R, Bjornson R, Kirschfeld K, Mismer D, Rubin GM, Smith DP, Socolich M, Zuker CS. 1992. Ectopic expression of ultraviolet-rhodopsins in the blue photoreceptor cells of *Drosophila*: visual physiology and photochemistry of transgenic animals. J Neurosci 12:3862–3868.

Fischbach KF. 1983. Neural cell types surviving congenital sensory deprivation in the optic lobes of *Drosophila melanogaster*. Dev Biol 95:1–18.

Fischbach KF, Dittrich APM. 1989. The optic lobe of *Drosophila melanogaster*. I. A Golgi analysis of wild-type structure. Cell Tissue Res 258:441–475.

Fischbach KF, Lyly-Hünerberg I. 1983. Genetic dissection of the anterior optic tract of *Drosophila melanogaster*. Cell Tissue Res 231:551–563.

Gilbert C, Strausfeld NJ. 1991. The functional organization of male-specific visual neurons in flies. J Comp Physiol [A] 169:395–411.

Gilbert C, Strausfeld NJ. 1992. Small-field neurons associated with oculomotor and optomotor control in muscoid flies: functional organization. J Comp Neurol 316:72–86.

Gronenberg W, Strausfeld NJ. 1991. Descending pathways connecting the male-specific visual system of flies to the neck and flight motor J Comp Physiol [A] 169:413–426 [erratum, J Comp Physiol [A] 1992;170(1): 128].

Haag J, Borst A. 2001. Recurrent network interactions underlying flow-field selectivity of visual interneurons. J Neurosci 21:5685–5692.

Haag J, Borst A. 2004. Neural mechanism underlying complex receptive field properties of motion-sensitive interneurons. Nat Neurosci 7:628–634.

Harrison JB, Chen HH, Sattelle E, Barker PJ, Huskisson NS, Rauh JJ, Bai D, Sattelle DB. 1996. Immunocytochemical mapping of a C-terminus anti-peptide antibody to the GABA receptor subunit, RDL in the nervous system in *Drosophila melanogaster*. Cell Tissue Res 284:269–278.

Hausen K, Egelhaaf M. 1989. Neural mechanisms of visual course control

in insects. In: Stavenga DG, Hardie RC, editors. Facets of vision. Heidelberg: Springer. p 391–424.

Hayashi S, Ito K, Sado Y, Taniguchi M, Akimoto A, Takeuchi H, Aigaki T, Matsuzaki F, Nakagoshi H, Tanimura T, Ueda R, Uemura T, Yoshihara M, Goto S. 2002. GETDB, a database compiling expression patterns and molecular locations of a collection of Gal4 enhancer traps. genesis 34:58–61.

Homberg U, Würden S. 1997. Movement-sensitive, polarization-sensitive, and light-sensitive neurons of the medulla and accessory medulla of the locust, *Schistocerca gregaria*. J Comp Neurol 386:329–346.

Homberg U, Hofer S, Pfeiffer K, Gebhardt S. 2003. Organization and neural connections of the anterior optic tubercle in the brain of the locust, *Schistocerca gregaria*. J Comp Neurol 462:415–430.

Ibbotson MR, Maddess T, DuBois R. 1991. A system of insect neurons sensitive to horizontal and vertical image motion connects the medulla and midbrain. J Comp Physiol [A] 169:355–367.

Ito K, Urban J, Technau GM. 1995. Distribution, classification, and development of *Drosophila* glial cells in the late embryonic and early larval ventral nerve cord. Rouxs Arch Dev Biol 204:284–307.

Ito K, Awano W, Suzuki K, Hiromi Y, Yamamoto D. 1997. The *Drosophila* mushroom body is a quadruple structure of clonal units each of which contains a virtually identical set of neurones and glial cells. Development 124:761–771.

Ito K, Suzuki K, Estes P, Ramaswami M, Yamamoto D, Strausfeld NJ. 1998. The organization of extrinsic neurons and their implications in the functional roles of the mushroom bodies in *Drosophila melanogaster* Meigen. Learn Mem 5:52–77.

Ito K, Okada R, Tanaka NK, Awasaki T. 2003. Cautionary observations on preparing and interpreting brain images using molecular biology-based staining techniques. Microsc Res Tech 62:170–186.

Kalb J, Nielsen T, Fricke M, Egelhaaf M, Kurtz R. 2004. In vivo two-photon laser-scanning microscopy of Ca2+ dynamics in visual motion-sensitive neurons. Biochem Biophys Res Commun 316:341–347.

Kimura K, Ote M, Tazawa T, Yamamoto D. 2005. *Fruitless* specifies sexually dimorphic neural circuitry in the *Drosophila* brain. Nature 438: 229–233.

Krapp HG, Hengstenberg R. 1996. Estimation of self-motion by optic flow processing in single visual interneurons. Nature 384:463–466.

Krapp HG, Hengstenberg R, Egelhaaf M. 2001. Binocular contributions to optic flow processing in the fly visual system. J Neurophysiol 85:724–734.

Loesel R, Homberg U. 2001. Anatomy and physiology of neurons with processes in the accessory medulla of the cockroach *Leucophaea maderae*. J Comp Neurol 439:193–207.

Meinertzhagen IA, Hanson TE. 1993. The development of the optic lobe. In: Bate M, Martinez-Arias A, editors. The development of *Drosophila melanogaster*. Cold Spring Harbor, NY: Cold Spring Harbor Laboratory Press. p 1363–1491.

Milde JJ. 1993. Tangential medulla neurons in the moth *Manduca sexta*. Structure and responses to optomotor stimuli. J Comp Physiol [A] 173:783–799.

Morales J, Hiesinger PR, Schroeder AJ, Kume K, Verstreken P, Jackson FR, Nelson DL, Hassan BA. 2002. *Drosophila* fragile X protein, DFXR, regulates neuronal morphology and function in the brain. Neuron 34:961–972.

Nässel DR. 1988. Serotonin and serotonin-immunoreactive neurons in the nervous system of insects. Prog Neurobiol 30:1–85.

Power ME. 1943. The brain of *Drosophila melanogaster*. J Morphol 72:517–559.

Power ME. 1946. The antennal centers and their connections within the brain of *Drosophila melanogaster*. J Comp Neurol 85:485–518.

Renn SC, Park JH, Rosbash M, Hall JC, Taghert PH. 1999. A pdf neuropeptide gene mutation and ablation of PDF neurons each cause severe abnormalities of behavioral circadian rhythms in *Drosophila*. Cell 99:791–802.

Robertson HM, Preston CR, Phillis RW, Johnson-Schlitz DM, Benz WK, Engels WR. 1988. A stable genomic source of P element transposase in *Drosophila melanogaster*. Genetics 118:461–470.

Salcedo E, Huber A, Henrich S, Chadwell LV, Chou WH, Paulsen R, Britt SG. 1999. Blue- and green-absorbing visual pigments of Drosophila: ectopic expression and physiological characterization of the R8 photoreceptor cell-specific Rh5 and Rh6 rhodopsins. J Neurosci 19:10716–10726.

Sinakevitch I, Douglass JK, Scholtz G, Loesel R, Strausfeld NJ. 2003. Conserved and convergent organization in the optic lobes of insects and isopods, with reference to other crustacean taxa. J Comp Neurol 467: 150–172.

Single S, Borst A. 1998. Dendritic integration and its role in computing image velocity. Science 281:1848–1850.

Stach S, Benard J, Giurfa M. 2004. Local-feature assembling in visual pattern recognition and generalization in honeybees. Nature 429:758–761.

Stocker RF, Lienhard MC, Borst A, Fischbach KF. 1990. Neuronal architecture of the antennal lobe in *Drosophila melanogaster*. Cell Tissue Res 262:9–34.

Stocker RF, Heimbeck G, Gendre N, de Belle JS. 1997. Neuroblast ablation in *Drosophila* P[GAL4] lines reveals origins of olfactory interneurons. J Neurobiol 32:443–456.

Strausfeld NJ. 1976. Atlas of an insect brain. Heidelberg: Springer.

Strausfeld NJ. 1991. Structural organization of male-specific visual neurons in calliphorid optic lobes. J Comp Physiol [A] 169:379–393.

Strausfeld NJ, Gilbert C. 1992. Small-field neurons associated with oculomotor control in muscoid flies: cellular organization in the lobula plate. J Comp Neurol 316:56–71.

Strausfeld NJ, Gronenberg W. 1990. Descending neurons supplying the neck and flight motor of Diptera: organization and neuroanatomical relationships with visual pathways. J Comp Neurol 302:954–972.

Strausfeld NJ, Hausen K. 1977. The resolution of neuronal assemblies after cobalt injection into neuropil. Proc R Soc Lond B 199:463–476.

Strausfeld NJ, Lee JK. 1991. Neuronal basis for parallel visual processing in the fly. Vis Neurosci 7:13–33.

Strausfeld NJ, Kong A, Milde JJ, Gilbert C, Ramaiah L. 1995. Oculomotor control in calliphorid flies: GABAergic organization in heterolateral inhibitory pathways. J Comp Neurol 361:298–320.

Tanaka NK, Awasaki T, Shimada T, Ito K. 2004. Integration of chemosensory pathways in the *Drosophila* second-order olfactory centers. Curr Biol 14:449–457.

Tang S, Wolf R, Xu S, Heisenberg M. 2004. Visual pattern recognition in *Drosophila* is invariant for retinal position. Science 305:1020–1022.

Verkhusha VV, Otsuna H, Awasaki T, Oda H, Tsukita S, Ito K. 2001. An enhanced mutant of red fluorescent protein DsRed for double labeling and developmental timer of neural fiber bundle formation. J Biol Chem 276:29621–29624.

Wicklein M, Strausfeld NJ. 2000. Organization and significance of neurons that detect change of visual depth in the hawk moth *Manduca sexta*. J Comp Neurol 424:356–376.

Wolff T, Ready DF. 1993. Pattern formation in the *Drosophila* retina. In: Bate M, Martinez-Arias A, editors. The development of *Drosophila melanogaster*. Cold Spring Harbor, NY: Cold Spring Harbor Laboratory Press. p 1277–1325.

Wong AM, Wang JW, Axel R. 2002. Spatial representation of the glomerular map in the *Drosophila* protocerebrum. Cell 109:229–241.

Yoshihara M, Ito K. 2000. Improved Gal4 screening kit for large-scale generation of enhancer-trap strains. Drosophila Information Service 83:199–202.